

LABORATORY MEASUREMENT OF SHEAR STRENGTH  
AND RELATED ACOUSTIC PROPERTIES

CENTRE FOR NEWFOUNDLAND STUDIES

**TOTAL OF 10 PAGES ONLY  
MAY BE XEROXED**

(Without Author's Permission)

ZHUO-HUA TANG







**Laboratory Measurement of Shear Strength  
and  
Related Acoustic Properties**

BY

© **Zhuo-hua Tang, B. Eng., M. Eng.**

A Thesis Submitted To the School of Graduate Studies  
in Partial Fulfillment of the Requirements for the Degree of  
Master of Engineering

Faculty of Engineering and Applied Science  
Memorial University of Newfoundland  
April 29, 1993

St. John's

Newfoundland

Canada



National Library  
of Canada

Acquisitions and  
Bibliographic Services Branch

395 Wellington Street  
Ottawa, Ontario  
K1A 0N4

Bibliothèque nationale  
du Canada

Direction des acquisitions et  
des services bibliographiques

395, rue Wellington  
Ottawa (Ontario)  
K1A 0N4

Tel: 613-993-9234

Tel: 613-993-9234

The author has granted an irrevocable non-exclusive licence allowing the National Library of Canada to reproduce, loan, distribute or sell copies of his/her thesis by any means and in any form or format, making this thesis available to interested persons.

L'auteur a accordé une licence irrévocable et non exclusive permettant à la Bibliothèque nationale du Canada de reproduire, prêter, distribuer ou vendre des copies de sa thèse de quelque manière et sous quelque forme que ce soit pour mettre des exemplaires de cette thèse à la disposition des personnes intéressées.

The author retains ownership of the copyright in his/her thesis. Neither the thesis nor substantial extracts from it may be printed or otherwise reproduced without his/her permission.

L'auteur conserve la propriété du droit d'auteur qui protège sa thèse. Ni la thèse ni des extraits substantiels de celle-ci ne doivent être imprimés ou autrement reproduits sans son autorisation.

ISBN 0-315-91634-6

Canada

Dedicated to my parents

and

my sweetheart Lianlian

献给艰辛养育我的父母

献给我深爱的温情美丽的霞

## Abstract

The general purpose of this research is to pursue the correlation between acoustic properties and strength properties of sands. Conventional methods for correlating these characteristics rely on in-situ measurements of the wave velocity and shear strength. These measurements are subject to error from contamination by many unknown influences. A combined laboratory acoustic-triaxial testing equipment was developed to study reliably the interrelationship between shear strength and shear wave velocity by using piezoelectric ceramic benders to measure shear wave velocity in the triaxial tests. In processing the wave signals, the Hilbert transform technique was applied to precisely determine the wave propagation time.

An unified stress-strain model is proposed for predicating sand behavior under loading conditions. It is found that the popular hyperbolic equation is a special case of the new model that can be applied to sands with a wide range of relative densities.

Shear wave velocity increases with increasing confining pressure but decreases with increasing void ratio. It is found that shear wave velocity increases with increasing axial strain until reaching its peak strength and then drops. The rate of decrease depends on the type of sand and confining pressure.

The microstructural analyses and experimental results indicate that the shear wave velocity-axial strain relationship follows the same mechanism controlling stress-strain

behavior of sands. Therefore the new stress-strain model is modified further according to experimental results to correlate shear wave velocity and shear strength. Unambiguous results in shear wave velocity have been established as a function of stress ratio and axial strain. The comparisons between model and measured data indicate that the proposed equation can describe well wave velocity changes with stress and strain.

## Acknowledgements

I would like to take this opportunity to express my sincere appreciation from the bottom of my heart to my supervisor Dr. Jack I. Clark for his excellent guidance in the research, generous financial support and great patience and encouragement, which will be remembered forever.

I wish to express my gratitude to Dr. J. Guigne and Mr. V. Chin of Guigne International Ltd. for their valuable suggestions and discussions. Their assistance to me is gratefully acknowledged.

Appreciation and gratitude are extended to Ms. J. Whittick, Ms. R. Healey, Ms. P. LeFeuvre and other C-CORE staff in the Technical Support Group and Administration Group.

Special thanks to Mr. A. Bursey in the Structural Lab for his help and assistance in my experiments. I am very thankful to Dr. P. Morin and Dr. T. R. Chari for their discussions and references.

NSERC grants for the triaxial equipment and data acquisition system are gratefully acknowledged.

I would like to thank some of my fellow graduate students: Xia Wu, M. Paulin, F. Zhu for their helpful discussion and assistance in my experiments.

*THE TRUTH IS THE WHOLE*

- Hegel

# Contents

<b>Abstract</b>	<b>i</b>
<b>Acknowledgements</b>	<b>iii</b>
<b>Contents</b>	<b>v</b>
<b>List of Figures</b>	<b>viii</b>
<b>List of Tables</b>	<b>x</b>
<b>List of Symbols</b>	<b>xi</b>
<b>1 Introduction</b>	<b>1</b>
1.1 General . . . . .	1
1.2 Objectives . . . . .	5
<b>2 Literature Review and Methodology</b>	<b>8</b>
2.1 Overview . . . . .	8
2.2 Shear Waves and Compressional Waves . . . . .	10
2.3 Shear Strength of Sands . . . . .	12
2.4 Correlations: the state-of-the-art . . . . .	19

2.4.1	methodology . . . . .	19
2.4.2	acoustic properties vs. physical properties . . . . .	21
2.4.3	acoustic properties vs. stress and strain . . . . .	22
2.4.4	acoustic properties vs. shear strength . . . . .	26
2.4.5	impedance vs. geotechnical properties . . . . .	31
2.5	Discussion and Summation . . . . .	32
2.5.1	strain rate . . . . .	32
2.5.2	strain level . . . . .	34
2.5.3	in-situ and laboratory techniques . . . . .	35
2.5.4	summation . . . . .	36
<b>3</b>	<b>Equipments, Materials and Experimental Program</b>	<b>37</b>
3.1	Triaxial System . . . . .	38
3.1.1	General Description . . . . .	38
3.1.2	Triaxial Cell . . . . .	40
3.1.3	Control Panel . . . . .	41
3.2	Hardware and Software for Data Acquisition and Control . . . . .	44
3.2.1	Hardware . . . . .	44
3.2.2	Software . . . . .	45
3.3	Acoustic Measurement Equipment . . . . .	47
3.3.1	General Description . . . . .	47
3.3.2	Installation of the Benders in the Triaxial Cell . . . . .	48
3.3.3	Measurement of Shear Wave Velocity . . . . .	50
3.3.4	Discussion . . . . .	56
3.4	Materials Tested . . . . .	57

3.5	Experimental Program . . . . .	60
<b>4</b>	<b>Hilbert Transform and Propagation-time Estimation</b>	<b>65</b>
4.1	Introduction . . . . .	65
4.2	Hilbert Transform . . . . .	67
4.3	Instrumentation and Data Analysis . . . . .	69
<b>5</b>	<b>Experiment Results and Analyses</b>	<b>72</b>
5.1	Stress-Strain Relationship . . . . .	73
5.2	Acoustic Experiments . . . . .	80
5.3	Correlation of Strength and Wave Velocity . . . . .	88
<b>6</b>	<b>Summary and Conclusions</b>	<b>91</b>
	<b>References</b>	<b>94</b>
	<b>Appendix</b>	<b>103</b>
<b>A</b>	<b>Test Procedures and Calibration of Transducers</b>	<b>103</b>
A.1	Test Procedures . . . . .	104
A.2	Transducer Calibration . . . . .	117
<b>B</b>	<b>Experimental Results</b>	<b>120</b>
B.1	Strength Tests . . . . .	121
B.2	Acoustic Data Samples . . . . .	158
B.2.1	measurements by oscilloscope . . . . .	159
B.2.2	measurements by Hilbert transform . . . . .	164
B.3	Stress-strain-shear wave velocity Data . . . . .	178

# List of Figures

2.1	Soil Transfer System . . . . .	20
2.2	Diagrammatic Model Adopted for the Present Study . . . . .	21
2.3	$V_s$ vs. Strain for a Sand in the Triaxial Cell(after Schultheiss, 1983) . . . . .	25
2.4	General Relation between Porosity and Strength(after Keller, 1979) . . . . .	27
2.5	Shear Strength vs. $V_p$ (after Nacci et al, 1974) . . . . .	29
2.6	Dynamic Shear Modulus vs. Shear Strength(after Chao & Chiang, 1978) . . . . .	31
3.1	Digital Tritest 50 and Control Panel . . . . .	39
3.2	Triaxial Cell Assembly . . . . .	42
3.3	Flow Chart of Control Panel. In the figure, M1 ..M4 indicate pressure meters; B1...B4 indicate pressure regulators; V1...V7 indicate valve. . . . .	43
3.4	Layout of Data Acquisition/Control System . . . . .	46
3.5	Soil Sample with Bender Elements at Bottom and Cap . . . . .	49
3.6	Installation of Bender Element . . . . .	51
3.7	Setup for Acoustic Measurement in the Triaxial Test . . . . .	53
3.8	Electronic Equipment Used in the Acoustic-triaxial Test . . . . .	54
3.9	Record of Traveling Time and Shear Wave Received with an Oscilloscope . . . . .	55
3.10	Polarity of Shear Wave Arrival . . . . .	57
3.11	Typical Waveform(DT363) Recorded by Plotter . . . . .	58

3.12 Particle Size Distribution Curves of the Soils Tested . . . . .	62
4.1 Cross-correlation to Find Travel Time . . . . .	69
4.2 Propagation Time Estimated by Hilbert Transform. The envelope curve indicates propagation time $\Delta T = 212\mu s$ . . . . .	71
5.1 Effect of Confining Pressure on Strength . . . . .	74
5.2 Effect of Relative Density on Strength . . . . .	76
5.3 Effect of Grain Size on Strength . . . . .	76
5.4 Test Data(DT262) and Modelling Curves . . . . .	78
5.5 Comparison of Model and Test Data( $D_r=80\%$ ) . . . . .	78
5.6 Comparison of Model and Test Data( $\sigma_3=100\text{KPa}$ ) . . . . .	79
5.7 Effect of Void Ratio and Confining Pressure on Velocity . . . . .	82
5.8 Effect of Axial Strain and Confining Pressure on Shear Wave Velocity .	83
5.9 Effect of Relative Density and Type of Sands on Shear Wave Velocity .	85
5.10 Stress-Strain-Velocity Relation(DT561 and DT283) . . . . .	86
5.11 Comparison of Model and Test Data(DT561 and DT283) . . . . .	90

# List of Tables

2.1 In-situ and Laboratory Strength Tests . . . . .	16
2.2 Comparison of In-situ, Laboratory and Analytical Approaches . . . . .	17
2.3 Physical Variables Affecting Soil Strength(after Saiki, 1986) . . . . .	22
3.1 Index Properties of Soils Tested . . . . .	59
3.2 Acoustic Triaxial Test Program . . . . .	63
3.3 Porosity and $W_s$ Used in the Test Program . . . . .	64
5.1 Effect of Signal Frequency . . . . .	80

## List of Symbols

$V_p$	compressional wave velocity
$V_s$	shear wave velocity
$K$	bulk modulus
$G$	shear modulus
$\epsilon$	axial strain
$\epsilon_f$	axial strain at failure
$\gamma$	shear strain
$G_{max}$	shear modulus corresponding to $\gamma = 10^{-6}$
$D$	constrained modulus
$\rho$	material density
$m_v$	coefficient of volume change
$E$	Young's modulus
$V_c$	compressional wave velocity in a rod
$\nu$	Poisson's ratio
$\phi$	the angle of internal friction
$\phi_{avg}$	average value of internal friction angle
$\phi_s$	component of $\phi$ due to soil particle surface roughness
$\phi_r$	component of $\phi$ due to reorientation of soil particles
$\phi_d$	component of $\phi$ due to dilatancy

$\phi_{deg}$	component of $\phi$ due to particle degradation
$\epsilon_c$	elastic strain
$\epsilon_p$	plastic strain
$\tau_f, q, q_f, q_o$	shear strength
$q_{max}$	maximum deviator stress
$c$	cohesion
$\gamma_w$	unit weight of water
$\sigma$	total normal stress
$\sigma'$	effective normal stress
$\sigma'_o$	average effective confining pressure
$\sigma_f$	total normal stress at failure plane
$\sigma_1, \sigma_2, \sigma_3$	total principal stresses
$\sigma'_1, \sigma'_2, \sigma'_3$	effective principal stresses
$\sigma'_m$	$(\sigma'_1 + \sigma'_2 + \sigma'_3)/3$ , mean principal effective stress
$\sigma_o$	mean principal stress
$D_r$	relative density
$y(t)$	acoustic input signal
$x(t)$	acoustic output signal
$L_o$	sample height, in mm
$L$	$L_o - 2l$ , in mm
$r$	sample radius, in mm
$W_s$	soil solid particles weight
$v$	$\pi r^2 L$ , sample volume, in $mm^3$
$T$	wave propagation time

$f(\sigma, \epsilon)$	function of stress and strain
$\tau(\sigma, \epsilon)$	function of strength characteristics
$\psi$	lumped parameter of physical properties
$S(\psi)$	function of physical properties
$n$	porosity
$e$	void ratio
$K_2$	parameter defining $G$ as a function of strain and pressure
$V$	sound speed
$S_u$	undrained strength
$c_u$	unconfined compressive strength
$D_{10}$	grain diameter at 10% passing
$D_{30}$	grain diameter at 30% passing
$D_{60}$	grain diameter at 60% passing
$C_u$	$\frac{D_{60}}{D_{10}}$ , coefficient of uniformity
$C_c$	$\frac{(D_{30})^2}{(D_{10})(D_{60})}$ , coefficient of curvature
$e_{min}$	void ratio of soil in densest condition
$e_{max}$	void ratio of soil in loosest condition
$G_s$	specific gravity of soil solids
DT363	symbol for the test series; The first digital refers to the type of sand. DT363 here is sand #3; The second digital refers to relative density. DT363 here is 60%; The third digital refers to confining pressure. DT363 here is 300KPa. If the third digital is missing, the confining pressure is 50KPa.
$Z$	acoustic impedance

$S$	vane shear strength
$W_L$	liquid limit
$\tilde{X}(t)$	Hilbert transform
$P_a$	atmospheric pressure
$\sigma'_a$	normal effective stress in the direction of wave propagation
$\sigma'_p$	normal effective stress in the direction of particle vibration
$\sigma'_{av}$	$(\sigma'_a + \sigma'_p)/2$
$A$	a parameter depending on particle shape and void ratio
$F(e)$	a function of particle shape and void ratio

# Chapter 1

## Introduction

Unfortunately, the research activities in soil mechanics had one undesirable psychological effect. They diverted the attention of many investigators and teachers from manifold limitations imposed by nature on the application of mathematics to problems in earthwork engineering. As a consequence, more and more emphasis has been placed on refinements in sampling and testing and on those very few problems that can be solved with accuracy.

- Terzaghi & Peck[1]

### 1.1 General

In this era of intensive ocean resource exploitation, there has been an increased interest in the rapid and reliable determination of the geotechnical engineering properties of the seabed, for the development of offshore facilities in a secure and cost-effective way requires a knowledge of the physical and mechanical properties of the seabed materials. However, the relative inaccessibility of the marine sediments makes the required engineering parameters difficult to assess using traditional geotechnical testing procedures such as sample recovery, penetration testing, pressuremeter testing, and vane shear testing. These geotechnical techniques for site investigation can only supply limited information about the seabed because of the small quantities of sampling

or testing due to the high cost. In addition, those methods show significant variations in soil properties even at the same site due to sample disturbance and many other unknown factors influencing different testing methods. These asperities have led to an intensive development of in-situ geophysical methods for geotechnical applications.

Conventional geophysical techniques[2, 3], for instance, seismic surveys and bore-hole measurements, have been used for many years to investigate the nature of the seabed and the sedimentary structures. However, although substantial amounts of research have been carried out, quantitative data from seismic surveys is not generally useful for predicting the response of a sediment to imposed loadings. An alternative geophysical approach to acquire and derive geotechnical data has emerged in recent years. That is the application of acoustic methods which have recently attracted considerable attention in soil exploration. Because of the ease with which sound can be transmitted in seawater, acoustic techniques have provided a wide range of tools for accumulating knowledge of the environment below the seabed surface. The sedimentary matrix influences the behavior of the sound propagation and hence furnishes the basis for correlation of geotechnical properties and acoustic responses. The recently developed non-linear acoustic technique for remotely sensing the ocean floor has been especially useful to better evaluate the properties of marine sediments[4]. The non-linear acoustic system is more potent than ordinary acoustic methods and may result in more characteristic correlations, both fundamental and empirical, between acoustic wave velocities and geotechnical parameters.

In laboratory acoustic geotechnical tests, a new combined technique has been

developed[5, 6]. The core part of this technique is the piezoceramic bender element that can generate shear waves in soils. The benders can be mounted in various conventional geotechnical apparatus such as resonant column, triaxial apparatus and oedometers. The bender technique has been widely used so far in the geotechnical laboratories because of its low-cost, flexibility and controllable physical characteristics.

Although the acoustic technique is unlikely to provide direct measurements of all properties of soils, quantitative physical information about marine sediments can be estimated through the acoustic wave propagation in the seafloor, and the mechanical properties can be inferred from these fundamental physical properties[7]. In addition, two advantages make the non-linear acoustic approach fairly attractive in marine geotechnical engineering[8]. First, it remotely senses the seabed. Usually, the properties of a soil is measured by certain devices either in-situ or in the laboratory. Those bulky devices must be in contact with the soil, which disturbs or even destroys the soil structures and thereby changing the strength and other properties of the soil. Nevertheless, the acoustic technique with non-disturbance allows iterative surveys of seafloor characteristics and hence presents the possibility of monitoring sediment properties in time series. Second, because of its easy deployment and economical operation, it is possible to quickly make large numbers of spatially continual measurements. Undoubtedly, acoustic method is of economical and engineering significance in measuring in-situ geotechnical properties quickly.

The application of acoustics to seabed investigations at Memorial University of Newfoundland can be dated back to 1978[9, 10]. At present, physical property identi-

fication of sediments by their acoustic properties has been increasingly undertaken at the Center for Cold Ocean Resource Engineering(C-CORE)[11, 12, 13]. Based on the concept by Guigne[14], a new non-linear acoustic site surveying technique was developed. It is called IMAP(interactive marine acoustic probe). The IMAP probe is an intelligent stationary geophysical tool designed to measure the properties of the seabed with unprecedented resolution in time and space. In the Fall of 1990, a comprehensive geotechnical program was commissioned offshore Terrenceville, Newfoundland by C-CORE[15]. Also, several in situ acoustic measurements for soils were made using the IMAP. The objective of this investigation was to acquire information on soil properties to provide correlations for the IMAP results obtained during the acoustic survey. At present the IMAP uses only the transmission of compression waves to image the seabed.

Nevertheless, field studies such as these at Terrenceville are still very expensive and often yield less than satisfactory results due to the uncontrolled conditions. On the other hand, as aforementioned, up to now, most acoustic-geotechnical measurements are aimed at determining the soil physical properties such as porosity, density, grain size, subsurface geological profile, and a few mechanical parameters. The correlations of acoustic properties and shear strength of soils have until recently received little consideration in offshore geotechnical geophysics. As we know, shear strength is one of the most important mechanical properties of soils, especially in the practice of marine geotechnical engineering. Regarding the importance of the shear strength of a soil to the geotechnical engineer, Schmertmann claimed "If they could know only one property, many would probably choose the insitu shear strength"[16]. Shear strength

was even ranked the highest priority for U.S. federal funding of seafloor engineering research[17]. Because of the weightiness of this parameter in the everyday practice of geotechnical engineering, some direct or indirect attempts have been made to correlate acoustic properties with shear strength but generally without satisfactory results. This problem may be that reliable and accurate in-situ shear strength values are not easily obtained. Actually, most of the previous comparisons were carried out between sound wave velocity and the shear strengths measured by vane shear testing or other in-situ methods.

Laboratory testing can provide a degree of flexibility, control, and economy not usually achieved with in-situ testing[18]. To assess the potential value of the acoustic method and broaden its applications in seabed sediments investigations, more inclusive laboratory experiments are required to examine the relationships between acoustic and mechanical properties of soils. Laboratory testing, correlation, and verification is an essential complement to the field work. The theoretical and empirical constitutive relations should be established through laboratory studies with well defined, directly controllable boundary conditions and uniformity of stresses and strains within the sample.

## 1.2 Objectives

Theoretically, there is no doubt that geophysical and geotechnical properties of a soil may be remotely derived using acoustics. Practically, if the propagation velocity of a mechanical force in soil could be related to the strength of a soil, it would offer a non-intrusive non-destructive method of characterizing soil strength. In the light

of non-linear acoustic application achievements in geotechnical engineering, it seems a quite promising undertaking to develop such a remote method for determining the strength of soils.

As a preliminary investigation, and also in order to provide geotechnical laboratory experimental data for the proposal being developed at C-CORE for the incorporation of a shear wave source into the IMAP technology, the principal objective of this research is to investigate relationships between shear wave velocity and shear strength characteristics of sands in the laboratory using acoustic-triaxial testing, and further, to establish a constitutive model to predict soil behavior from the measurement of sound speeds only or vice versa. The effects of relative density, acoustic signal frequency and confining pressure are studied.

In order to better understand the acoustic behavior of sand when it is sheared, the most dependable way is to measure the shear strength and acoustic wave velocity simultaneously. To fulfill this function, a modified triaxial machine combined with piezoelectric ceramic transducers was constructed as a part of this research.

Accuracy in shear wave velocity data is essential in evaluating the dynamic response of soil. For reliable measurement of the shear wave velocity, it is necessary to correctly determine the travel time interval of the outgoing signal from the transmitter to the receiver. For this purpose, the Hilbert transform technique was employed to supplement the ordinary measurement using an oscilloscope.

Ultimately, this research is aimed at contributing to the development of practical in-situ measurement of shear strength using a rapid and economical acoustic method. The specific scope of this research may be grouped as follows:

1. Description of methodology. Literature survey of laboratory and in-situ measurements of shear strength; comparison of geophysical methods for geotechnical applications; correlation between geotechnical and acoustic properties of soils.
2. Chapter 3 describes the equipment modification and set up. Tested materials and the experimental program are also presented in the same chapter.
3. Introduction to the Hilbert transform and its performance in propagation-time estimation; comparison between conventional analog measurement and the Hilbert transform envelop.
4. Presentation of the major experimental results and analysis.
5. Summary and conclusions are presented in chapter 6. Recommendations for future research are also included in this chapter.
6. Details of experimental procedures, transducer calibration and some experimental results are included in the Appendices.

## Chapter 2

# Literature Review and Methodology

As is well known in soil mechanics, a necessary prerequisite for a successful application of a new finding is that the responsible engineer has a rather thorough understanding of the fundamentals of the new method, so that he is familiar with the assumptions on which the development is based and has a feeling for its limitations.

L. Bjerrum[19]

### 2.1 Overview

By their very essence, soils as porous media are composite and multiphase. The microscopic heterogeneity of soils induces a complex macroscopic physical behavior sensitive to slight variations of the solid structure, fluid content or external stress conditions. Because of these vicissitudes, it is very difficult to model soil behavior by synthesizing between the rigor of the laws of mechanics and the alleged disorder of porous soil. Being directed at untangling these predicaments, therefore, the acoustic technique becomes one of the surest means available for the remote investigation of soils. This approach plays a major role in the study of marine deposits. After decades

of research and development up to today's non-linear acoustic technique, it has been recognized that acoustic characteristics as measured in soils can provide information not only about the profiles of soil layering, but also about the physical properties, as well as some mechanical properties. Acoustic measurements provide direct information on compressional and shear wave velocities, Poisson's ratio, attenuation and impedance. In addition, if the sediment density is known, dynamic values of compressibility, shear modulus<sup>1</sup> and other elastic constants, and even permeability[20, 21] can be inferred.

However, although acoustic methods have been used extensively, they were in the past applied mostly to delineate the morphology or geometric image of the subsurface and evaluate porosity, grain size distribution and other spatial variabilities. In contrast, relatively little use has been made of acoustic waves for the determination of soil strength properties of direct interest to foundation designs and other geotechnical engineering problems. In this regard, not much data in the existing literature is available.

As to the shear strength of soils, it has been well documented through centuries of accumulation. The theory of shear strength occupies an important place in geotechnical engineering. The strength characteristic of soils is a compelling parameter with which an engineer has to deal in all aspects of geotechnical engineering. In ocean exploration, the rapid and accurate determination of shear strength of marine sediments is especially significant. Generally, two components, cohesion and friction contribute to the shearing strength of clay. For sand, only frictional resistance attributes to the shear strength.

---

<sup>1</sup>Or rigidity.

In order to focus on the acoustic-geotechnical interactions of porous earth media, we only use dry sands as testing materials in this study. The use of dry sands allow us to avoid many other influencing factors and concentrate on wave velocity-shear strength correlation. The following literature search relates mainly therefore to sands.

## 2.2 Shear Waves and Compressional Waves

In the applications of acoustics, usually two kinds of waves are considered to travel in the subsoil although at the surface Rayleigh waves exist. One is the compressional or dilatational wave<sup>2</sup>, sometimes also called longitudinal or  $P$  waves<sup>3</sup>, where  $P$  corresponds to primary because these are the fastest waves likely to propagate in an isotropic linear elastic medium. In the case of compressional waves, the particle movement is along the axis of wave propagation. In elastic theory, the  $P$  wave velocity is defined as follows:

$$V_p = \left[ \frac{K + \frac{4}{3}G}{\rho} \right]^{\frac{1}{2}} = \sqrt{\frac{D}{\rho}} = \sqrt{\frac{1}{\rho m_v}} \quad (2.1)$$

where  $K$  is the bulk modulus, or incompressibility;

$G$  is the shear modulus;

$D$  is the constrained modulus =  $K + 4G/3$ ;

$\rho$  is the material density;

$m_v$  is coefficient of volume change or unidimensional compressibility.

Compressional waves can propagate in both solids and fluids. However, it should be noted that, if the soil is saturated with fluid, there exists two different compressional

<sup>2</sup>Here the compressional wave velocity  $V_p$  is for an infinite elastic medium.  $V_p$  is different from the compressional wave velocity  $V_c$  in a rod where  $V_c = \sqrt{E/\rho}$ , where  $E$  is Young's modulus, equal to  $3K(1 - 2\nu)$ , or equal to  $2G(1 + \nu)$ .

<sup>3</sup>Symbols used in the thesis are defined where they first appear and are arranged alphabetically in the List of Symbols.

waves, one slow propagating through the the soil skeleton and one standard propagating through pore fluid[22]. However, the slower one is usually not significant. In the absence of fluid, they merge with the  $P$ -wave.

Another type of sound wave is the shear wave. Shear wave velocity is an important soil property for the evaluation of dynamic behavior of soils as well as static deformation of the ground. Shear waves are also called transverse or  $S$  wave, where  $S$  stands for secondary because they are slower than the  $P$  wave. In the shear wave, particle movement is perpendicular to wave propagation direction. Since fluid does not respond to shear forces,  $S$  wave can only propagate in the solid phase. Treated in elastic theory, the shear wave velocity is given by<sup>4</sup> :

$$V_s = \sqrt{\frac{G}{\rho}} \quad (2.2)$$

Note that bulk modulus  $K$  and shear modulus  $G$  bear on the following relationship:

$$K = G \frac{2(1 + \nu)}{3(1 - 2\nu)} \quad (2.3)$$

where  $\nu$  is Poisson's ratio. Therefore  $V_p/V_s$  can be written as a function of Poisson's ratio in the form:

$$\frac{V_p}{V_s} = \sqrt{\frac{2(1 - \nu)}{1 - 2\nu}} \quad (2.4)$$

It is seen from this equation that  $V_p$  and  $V_s$  are not independent parameters for a given material. Provided one of them and also Poisson's ratio is known, the other one can be obtained from equation(2.4). For engineering convenience, an empirical equation

---

<sup>4</sup>Most often, the shear modulus in equation(2.2) is written as  $G_{max}$  that has a special meaning in soil dynamics.  $G_{max}$  corresponds to the very small shear strain amplitude of about  $10^{-6}$  order.

known as the Christensen equation[23] was further developed:

$$\frac{V_p}{V_s} = \left[ 1 - 1.15 \left( \frac{1}{\rho} + \frac{1}{\rho^3} \right) \frac{1}{e/\rho} \right]^{\frac{1}{2}} \quad (2.5)$$

The Christensen equation relates  $P$ - and  $S$ - wave velocities with material density. Originally, this equation was not derived for marine sediments. However, it would be helpful in some cases to determine shear wave velocity  $V_s$  because shear wave arrival is usually more difficult to identify, especially in soils saturated with fluid, than the compression wave due to the low signal level or acoustic noise. There are many in-situ methods for measuring the shear wave velocity such as down-hole, up-hole, cross-hole, sonic logging and suspension logging [24, 25, 26].

Among shear waves and compressional waves, the compressional waves are more intricate and it is usually difficult to extract useful information from them. Of particular consequence is the shear wave. Shear wave velocity  $V_s$  is essentially dependent on the stiffness of the soil skeleton. Thereby,  $V_s$  might be connected with soil strength characteristics. In this research, only shear wave is used as a tool to correlate with geotechnical data.

## 2.3 Shear Strength of Sands

Because of different definitions, we have different points of strengths such as peak strength, yield strength, residual and creep strength, as well as drained and undrained strength[27]. Specifically, this research only considers the internal peak shear strength of dry sands. The source of shear strength of granular sands is believed to be the resistance against mutual displacements of those particles which are in mineral-to-

mineral contact. Described by the angle of internal friction  $\phi$ , the shear strength of dry sands can be separated into four independent components[28]:

$$\phi = \phi_s + \phi_r + \phi_d + \phi_{deg} \quad (2.6)$$

1. microscopic interlocking angle of particles,  $\phi_s$ , due to their surface roughness at grain-to-grain contact points;
2. interlocking angle of friction,  $\phi_r$ , due to restraints to relative particle movement or reorientation affected by adjacent particles;
3. dilatancy component  $\phi_d$ ; and
4.  $\phi_{deg}$  is attributable to particle degradation.

On the planes of weakness, a macroscopic failure will occur when the shear stress exceeds the total friction resistance. A slip surface or a series of slip surfaces are formed and larger particle movement within those zones is further enacted. This phenomenon is likely to occur when the shear strain reaches such a magnitude that a local reorientation of particles starts to take place. The total strain<sup>5</sup>  $\epsilon$  of a sand is often considered as having two attributes: an elastic strain,  $\epsilon_e$ , due to deformation of the individual particles; and a plastic strain,  $\epsilon_p$ , due to slippage between particles which causes irrecoverable displacements and changes in the micro-fabric of the grain arrangements.

The definition of failure has not been given in general terms. The simplest and the best known failure theory to constitute the behavior of soils is the Mohr-Coulomb theory. In 1766, Coulomb proposed that the shearing resistance which can be mobilized

---

<sup>5</sup>It could also be shear strain  $\gamma$  which will not be discussed in this research.

in a soil varied proportionally with the normal stress<sup>6</sup>  $\sigma$ , i.e., the strength envelope of a soil could be expressed by a straight line:

$$\tau_f = c + \sigma \tan \phi \quad (2.7)$$

where  $\tau_f$  = shear stress at failure, i.e., the shear strength;

$c$  = cohesion.

Within sands, the component of cohesion is extremely small or equal to zero. Therefore, the above equation takes the following form for cohesionless materials:

$$\tau_f = \sigma \tan \phi \quad (2.8)$$

From equation(2.8) we can obtain the failure condition equation using principal stresses:

$$\frac{(\sigma_1 - \sigma_3)_f}{(\sigma_1 + \sigma_3)_f} = \sin \phi \quad (2.9)$$

where  $\sigma_1$  and  $\sigma_3$  are principal stresses. Subscript  $f$  refers to the condition of failure.

The limitations of the Mohr-Coulomb theory can be readily seen. For example, it is observed that the frictional strength is influenced by the physical properties of the soil as well as by the loading and deformation states. Generally, the criterion governing the failure of soils is most likely a strain criterion. However, the above equations do not consider the effect of strains or volume changes that a sand experiences on its way to failure. In addition, the Mohr-Coulomb theory does not consider the effect of the intermediate principal stress  $\sigma_2$ . Nevertheless, most studies show that the Mohr-Coulomb theory does give satisfactory predictions for most sands. In this research, the Mohr-Coulomb theory is used to interpret triaxial data.

---

<sup>6</sup>In the text, we only use the expression of total stress. For effective stress, one prime symbol is used to indicate the difference, for example,  $\sigma'$ .

The strength parameters can be determined by in-situ and laboratory tests and analytical procedures or a combination of them. A series of in situ tests can be employed for this purpose, including penetration testing[29], pressuremeter testing[30, 31], and vane shear tests[32]. In addition to these standard tests, new methods have been developed to measure field performance. It is reported that the shear strength changes can be monitored by measuring pore water pressure[33]. Acoustic emissions in triaxial compression tests were also found to be related to strength characteristics[34, 35]. Some of those methods are listed in table(2.1). A summary of the advantages and disadvantages of these methodologies is given by Chaney et al[36] as shown in table(2.2).

Triaxial test may be used for a variety of determinations, for instance, consolidation, permeability parameters, wave velocity and so forth. But its main function widely used in laboratories is for measuring shear strength. Triaxial tests have some advantages such as relative simplicity, versatility and reliability[37]. However, after many years of usage, problems still remain, arising from errors in test procedures and difficulties in interpreting the results of laboratory data. Yong and Tabba[38] suggested that the intrinsic nature of soil and sampling and testing techniques are two major sources attributed to the random scatter of measured shear strength.

The conventional triaxial test involves the application of normal stresses to all the sides of cylindrical specimen of a soil. It is commonly assumed that the stress and strain relations are uniform throughout the specimens. Yet it is found that different conditions may exist near the ends of the specimen because of the restraining effects of

Table 2.1: In-situ and Laboratory Strength Tests

In-situ Methods		Laboratory Methods
borehole shear		triaxial test
plate bearing load		unconfined compression test
field direct shear		direct shear test
vane shear test		vane shear test
acoustic emission		acoustic emission
hydraulic fracturing		torsional shear
Iskymeter		
porewater pressure monitoring		
penetration	standard	
	quasi-static	
	dynamic	
	cone penetration	
	piezocone	
	fall-cone	
	acoustic penetrometer	
pressuremeter	Menard tricell type	
	self-boring type	
	OYO monocell type	
	TEXAM monocell type	
	stressprobe push-in type	
	cone-pressuremeter	
	Marchetti dilatometer	
	Fugro full-displacement	
	Cambridge highpressure dilatometer	

Table 2.2: Comparison of In-situ, Laboratory and Analytical Approaches

	In-situ tests	Laboratory Tests	Analytical Studies
Advantages	1. ability to measure existing in-situ soil strength by insertion of probe	1. ability to stimulate and control a variety of environmental and/or structural loads	1. ability to perform parametric and sensitivity studies
	2. ability to measure existing in-situ pressure by insertion of probe	2. ability to investigate phenomena occurring over longer time span than normal in-situ test	2. economic if computer program or theory exists
	3. ability to quantify sands, sensitive or quick clays, and soils containing free gas or significant dissolved gas by use of a probe inserted in the deposit	3. economic under certain conditions	3. ability to make predictions on future loading conditions
	4. ability to measure variations in density gradients in sediment using remote sensing techniques	4. provides fundamental parameters for analytical models	4. ability to investigate phenomena occurring over long time span
	5. ability to measure surface expression of soil deposits using remote sensing techniques	5. ability to perform parametric sensitivity studies	
	6. ability to measure initial in-situ stress conditions		
Disadvantages	1. insertion of probe in soil generates excess pore pressure if soil is saturated	1. boundary conditions imposed by test apparatus	1. requires calibration of analytical technique
	2. insertion of probe in soil causes localized disturbance	2. interpretation of scaled results to prototype application	2. development of task specific computer programs expensive and takes time
	3. interpretation difficult without adjacent soil samples	3. possible sample disturbance due to: a) fabric changes; b) stress relief; c) desiccation	3. availability of input parameters is limited
	4. control of boundary conditions either difficult or impossible		4. utilizes highly idealized models
	5. difficult and expensive to perform long-term studies		
	6. not possible to measure future environmental loadings		
	7. typically expensive		

the specimen cap and base[39]. Nonuniform distribution of stress is caused around the ends of the specimen. The distribution of strain is also nonuniform. The end effects can be neglected only if the failure band is outside the end-restraining zones of the specimen. In addition, membrane strength and the penetration of the membrane into the spaces between particles may cause some extra errors[40, 41].

Variations in sand behavior resulting from different methods of sample preparation have recently received considerable awareness. The friction angle  $\phi$  of cohesionless soils has conventionally been regarded as a property that depends primarily on the relative density  $D_r$  of the soil. But recent laboratory studies show significant differences in the behavior of sands having the same relative density prepared by different methods. Besides, in ordinary triaxial testing on solid cylinder specimens,  $\sigma_2$  is equal either to  $\sigma_1$  or to  $\sigma_3$  and only a jump rotation of  $90^\circ$  in the principal stress directions can be achieved. In spite of all these limitations, it is argued that the triaxial testing method is still a useful means to measure the strength and deformation characteristics of soils[42]. The same technique is employed in this research.

## **2.4 Correlations: the state-of-the-art**

### **2.4.1 Methodology**

With the increased need for a more diversified view of the characteristics of subsoils in order to solve geotechnical problems, greater accuracy and rapidity of in-situ measurements are required. This necessitation calls for research and development of correlations between geophysics and geotechnics. As a matter of fact, correlation techniques have long been employed in many fields of science and technology. Because

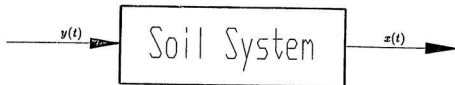


Figure 2.1: Soil Transfer System

of the complexity of the soil system, introducing correlation methodology into geotechnical engineering becomes more exigent[43]. We have known that some engineering characteristics of soils can be conjectured from index properties, and of particular importance is the shear strength [95]. With respect to the dynamic testing methods, we can use the illustration as shown in figure(2.1) to demonstrate the principles of correlation. In this study, we are interested in the acoustic approach. Therefore, let the input  $y(t)$  be the acoustic signal, for instance, a shear wave which will impose vibrations on elements in the soil system. If the properties of the soil and its constitutive relations between stress and strain were known, we could decide quantitatively the output signal  $x(t)$  which is a time dependent of the input signal.

Generally, the soil system is a "black box". What is known is only the input  $y(t)$  and output  $x(t)$  from which, hopefully, the mechanical properties of the "black box" are going to be determined. Specifically in the present study,  $x(t)$  is the measurement

of the shear wave propagation time  $T$  from which  $V_s$  and  $G$  can be derived, i.e.,

$$x(t) = T \rightarrow V_s = \frac{L}{T} \rightarrow G = \rho V_s^2 \quad (2.10)$$

where  $L$  is the travelling distance. In the real situation, the input to the soil system usually is a function  $f(\sigma, \varepsilon)$  of the mechanical parameters, stress  $\sigma$  and strain  $\varepsilon$ , not the acoustic signal  $y(t)$  that is applied only for intermediate purpose to initiate an output as an easily detectable and readily interpretable signal. From the output signal we can extract information relevant to the soil behavior under  $f(\sigma, \varepsilon)$ . Some engineering properties can be deduced from such acoustic measurements. Particularly, in this research only the strength characteristics  $\tau(\sigma, \varepsilon)$  is concerned. Therefore, we can use another a more practical miniature as shown in figure(2.2). That is the model used throughout this research. In the laboratory, a signal  $y(t)$  can be generated from piezoelectrical benders as used by the author or a resonant column device as used by Hardin and Richart[44]. The input  $f(\sigma, \varepsilon)$  is from the triaxial device in our laboratory. In figure(2.2),  $S(\psi)$  is a function of physical parameters(lumped into  $\psi$ ) of the soil system. There are many variables in  $\psi$  which affect the strength  $\tau(\sigma, \varepsilon)$  of soils. From a geotechnical point of view, variables which have relations with soil strength can be illustrated in table(2.3)[45]. In the table, the plasticity and moisture is applicable only to clay. Within the present study, only the relative density is considered. In summary, the above description can be charted simply as follows:

$$f(\sigma, \varepsilon) \xrightarrow{y(t)+S(\psi)} x(t) \xrightarrow{\text{correlation}} \tau(\sigma, \varepsilon) \quad (2.11)$$

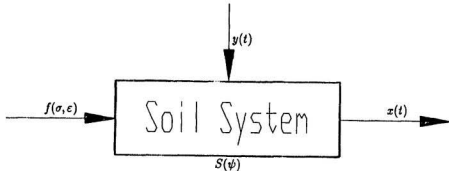


Figure 2.2: Diagrammatic Model Adopted for the Present Study

## 2.4.2 Acoustic properties vs. physical properties

With respect to the physical properties of soils, usually we refer to grain size, porosity<sup>7</sup>, moisture<sup>8</sup>, density. Sound velocity is an important physical parameter in determining those properties of soils. The relationship between sound velocity and porosity has received considerable attention in the past. Hardin and Richart[44] found that sound velocity varied linearly with void ratio and the presence of moisture in a sand reduced the velocity of the wave due to the mass of the water moving with the frame. They also reported that grain size had no effects on the shear wave velocity. However, several geophysicists established that a definite relationship existed between sound velocity and mean grain size which governs the bulk and textural properties of unconsolidated marine sediments[85, 87]. The general conclusion is that a decrease in porosity and moisture content is reflected by an increase in sound velocity. There is

<sup>7</sup>Or void ratio. Porosity  $n$  and void ratio  $e$  have the following relationship:  $n = e/(1 + e)$ .

<sup>8</sup>Or water content.

Table 2.3: Physical Variables Affecting Soil Strength(after Saiki, 1986)

Lumped $\psi$	Characteristics
1. Grain size	Grain size distribution, maximum grain size, mean grain size, coefficient of uniformity, shape of particles, content of fine fraction
2. Density	Void ratio, relative density, dry density, specific gravity
3. Plasticity	Liquid limit, plastic limit, shrinkage limit, plasticity index, consistency index
4. Moisture	Natural moisture content, degree of saturation
5. Texture	Type, proportion & structure of minerals and organic matters, orientation of particles
6. Stress History	Age of deposition, number & magnitude of stress change experience, weathering & physico-chemical effects

an increase in sound velocity as the wet density of the sediments increases. But dry density has little bearing on the transmission of sound through sediments.

### 2.4.3 Acoustic properties vs. stress and strain

Stress is an important factor that affects the magnitude of wave velocity. Several investigations have been conducted to study the relationship between shear wave velocity<sup>9</sup>  $V_s$  and the stress imposed on the soil. It was confirmed that the velocity is a function not only of the void ratio but also of the intergranular pressure[46]. Lawrence designed an ultrasonic pulse apparatus using a barium titanate crystal transducer[47]. With this device, sand was placed in a steel tube and a vertical load was applied while ultrasonic pulse was propagating through the sand. Similar devices were also

<sup>9</sup>Considering the equation (2.2),  $G_{max}$  and  $V_s$  will be used equally for the discussion in this chapter although  $V_s$  is the only direct measurement.

developed by other researchers[48, 49, 50] to investigate the dependency of acoustic wave velocities on the stresses in soil. Hardin and Richart pioneered a laboratory investigation method using a resonant column device[44]. They found both shear and compression wave velocities varied approximately between 1/2 and 1/4 power of the confining pressure, for round-grained sands:

$$V_s = (19.7 - 9.06e)(\sigma'_o)^{0.25} \quad (2.12)$$

and for angular-grained materials:

$$V_s = (18.4 - 6.2c)(\sigma'_o)^{0.25} \quad (2.13)$$

where  $e$  is the void ratio and  $\sigma'_o$  is the average effective confining pressure.

Instead of using void ratio, Edil and Luh[51] developed the following empirical relationship using the relative density  $D_r$  for uniform-sized dry sands:

$$G_{max} = 10^4 \times (0.305\sigma'_o^{0.5} \epsilon^{D_r} + 4.02\sigma'_o^{0.25} - 5.899) \quad (2.14)$$

where  $\sigma'_o$  is the mean principal stress. Shear wave velocity  $V_s$  was also empirically related by Seed and Idriss[52] to the mean principal effective stress  $\sigma'_m$  for sand:

$$G_{max} = 1000(\sigma'_m)^{0.5} K_2 \quad (2.15)$$

where  $\sigma'_m = \frac{\sigma'_1 + \sigma'_2 + \sigma'_3}{3}$ ;  $\sigma'_1$ ,  $\sigma'_2$  and  $\sigma'_3$  are effective principle stresses:

$K_2$  = parameter used in defining shear modulus as a function of shear strain and confining pressure.

This equation is similar to the foregoing ones. But it can be improved by considering the effect of shear strain although a specific description of the parameter  $K_2$  was not given.

From these results we can see that  $V_s$  depends only on the average stress. However, very recent studies indicate that  $V_s$  is influenced by the individual components of the confining pressures, i.e.,  $V_s$  depends about equally on the principal stresses in the direction of wave propagation and the direction of particle motion, and is relatively independent of the third principal stress[53, 54]. Yu and Richart[55] introduced a stress ratio  $k_n$  to consider this effect:

$$k_n = \frac{\frac{\sigma'_v}{\sigma'_a} - 1}{\left(\frac{\sigma'_v}{\sigma'_a}\right)_{max} - 1} \quad (2.16)$$

$$G_{max} = A F(e) Pa \left(\frac{\sigma'_{av}}{Pa}\right)^{0.5} (1 - 0.3k_n^{1.5}) \quad (2.17)$$

where parameters  $A$  and  $F(e)$  depend on particle shape and void ratio;  $Pa$  is atmospheric pressure;  $\sigma'_{av} = (\sigma'_a + \sigma'_p)/2$ , and  $\sigma'_a$  is the normal effective stress in the direction of wave propagation;  $\sigma'_p$  is the normal effective stress in the direction of particle vibration.

Strain developed in the soil is also a critical ingredient controlling wave velocities. Schultheiss[56, 57] conducted combined acoustic-triaxial tests and showed that  $V_s$  increased with axial strain and deviator stress, but a drop in  $V_s$  occurred when the sample is tested to failure as shown in figure(2.3). Nishio and Tamapki[58] also indicated that  $V_s$  increased at the initial stage of the triaxial compression tests, and decreased gradually until the failure of the specimen. They speculated that the increase and reduction in  $V_s$  with shear stress was principally caused by the rearrangement in the soil structure which could not be evaluated by the change of void ratio. These experiments are of significances in the sense of correlation of acoustic properties and shear strength of soils. Acoustic measurements are valid only when the deformations

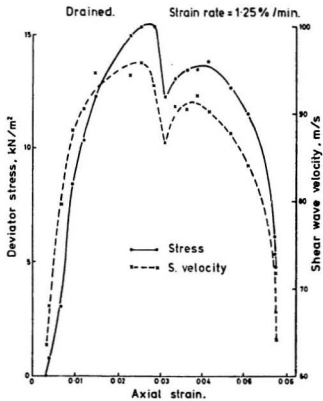


Figure 2.3:  $V_s$  vs. Strain for a Sand in the Triaxial Cell(after Schultheiss, 1983)

are very small. But shear strength is an indicator of large deformation. Those tests by Schultheiss and Nishio and Tamapki shed light on the possibility of relating these two different deforming properties.

Except for the above direct correlations between  $V_s$  and stress,  $V_s$  can even be correlated with  $N$ -values from standard penetration test to obtain dynamic properties of soils[59, 60]. In addition, correlations between acoustic shear or compression wave velocities and liquefaction of sand have increasingly attracted attention [61, 62, 63, 64]. These investigations, from a different perspective of deformation behavior, give us more insights about acoustic-geotechnical interrelations of soils.

#### 2.4.4 Acoustic properties vs. shear strength

As early as 1960, experiments on concrete showed that good correlation exists between compressive strength and pulse velocity[65], but there have been for some years no comprehensive experiments or theoretical considerations that relate the propagation velocity of mechanical waves to the strength of soils. However, it is well documented that the porosity is closely interrelated with strength[66]. Figure(2.4) shows the relation of porosity versus strength[67]. A unique relation seemingly exists between porosity and shear strength for each soil structure. Actually, porosity is a primary property governing sand strength and can be correlated with the angle of internal friction[68]. On the other hand, porosity has strong correlations with acoustic velocities as pointed out in the foregoing sections. The following can be used to illustrate their relationships:

$$\text{wave velocity}(V_s \text{ or } V_p) \approx \text{porosity} \approx \text{shear strength} \quad (2.18)$$

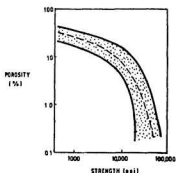


Figure 2.4: General Relation between Porosity and Strength(after Keller, 1979)

Further, in figure(2.3) it is quite obvious that the relation between shear wave velocity  $V_s$  and axial strain is similar to that between stress and strain. Intuitively, this similarity leads us to the consideration that certain inherent linkages between wave velocity and shear strength remain undiscovered. It is reasonable, therefore, to consider that acoustic properties, especially shear wave velocity  $V_s$ , is closely related to shear strength. Lee and Baecher[69] demonstrated from their studies that if the acoustic properties of a marine sediment was known, the preliminary estimates of the strength of the material could be derived. Sutton et al[70] explained higher velocities in their experiments as the combined result of shear strength and low effective porosity. More importantly, Bely et al[71] pointed out that an increase of cohesion caused  $V_s$  to rise and that the shear strength and the angle of internal friction were connected with  $V_s$ .

The earliest laboratory investigation of shear wave velocity and shear strength probably is that by D'Andrea[72]. He studied marine sediments with high porosity and de-

veloped empirical relations from which sediment shear strength can be predicted from the precise in-situ measurement of only sound speed:

$$V = 170.5 \frac{q}{q_f} + 4906 \quad (2.19)$$

and

$$V = 177.0 \frac{q_f}{q_o} + 4915 \quad (2.20)$$

where  $V$  is sound speed and  $q$  is shear strength. Subscripts  $f$  and  $o$  refer to conditions at failure and at primary consolidation respectively in consolidated undrained triaxial shear strength test. After testing the sediment cores, Buchan et al[73] concluded that sound velocity has a positive correlation with shear strength, i.e., the greater values of velocity correlate with the greater values of shear strength<sup>10</sup>. DeRoock and Cooper[74] reported a high degree of linear correlation between propagation velocity of an impact wave through the soil and the resistance to penetration of the cone into the soil. A higher penetration resistance corresponded with a higher propagation velocity. But they did not distinguish between shear waves and compression waves. A large number of in-situ tests were conducted by Horn et al[75] who plotted shear strength against sound velocity. The data fall into distinct groups. There is an overall increase in sound velocity as the shear strengths get larger. Seed and Idriss[52] observed that the ratio of shear modulus  $G = \rho V_s^2$  and undrained strength  $S_u$  of clay did not vary much:

$$\frac{G_{mar}}{S_u} = constant \quad (2.21)$$

From the survey of 39 in-situ samples, Deness et al[76] also obtained clear correlation between the velocity of sound and the undrained shear strength. Hara et al[77]

---

<sup>10</sup>They even found a reasonable correlation between shear strength and acoustic attenuation!

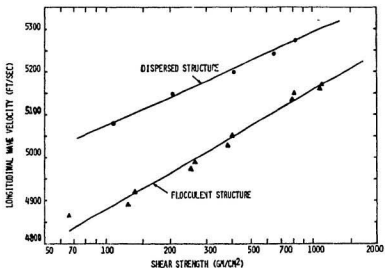


Figure 2.5: Shear Strength vs.  $V_p$  (after Nacci et al, 1974)

developed an empirical relation for clay:

$$G_{max} = 487(S_w)^{0.928} \quad (2.22)$$

This equation is similar to that by Seed and Idriss. Linear relationships also exist between compressional wave velocity and log shear strength as shown in figure(2.5)[78].

Recently, a more specific relationship between the static strength and the shear wave velocity was developed by Chae and Chiang[79] for lime- and lime-fly ash treated sands:

$$G_{max} = 13.867 + 0.419(\sigma_1 - \sigma_3) \quad (2.23)$$

where the strength data was obtained from triaxial compression tests at 138KPa confin-

ing pressure. The failure criterion was set at 1% axial strain. From the above equation we can see dynamic shear modulus  $G$  has a linear relationship with strength as shown in figure(2.6). Using results from triaxial and resonant column devices, Saxena et al[80] established a similar equation at 1% axial strain of static triaxial drained tests:

$$G_{max} = 72.47P_a + 1109.22(\sigma_1 - \sigma_3) \quad (2.24)$$

where  $P_a$  is atmospheric pressure. It should be recognized that valid applications of equations (2.23) and (2.24) are very limited because they were derived under special conditions. As an important index of shear strength, the angle of internal friction  $\phi$  was used by Zhang and Lin[81] for evaluating the correlation with shear wave velocity of tailings. They showed the following equation:

$$V_s = 0.012(\phi)^{2.743} \quad (2.25)$$

Unconfined compressive strength  $c_u$  of clay is also often used by engineers. It was related with shear wave velocity by Tonouchi et al [82]:

$$V_s = 134(c_u)^{0.433} \quad (2.26)$$

All of these investigations confirm further that shear wave velocity is a valuable geotechnical tool for correlation with strength parameters[83].

On the contrary, however, scatter still exists among test results. Lorimer et al[84] showed that the acoustic value of shear wave speed was about 45 times greater than that derived from the vane shear testing. From his in-situ investigation of cohesion and sound velocity, Hamilton[85, 86] indicated that there was no usable empirical relationship between sound velocity and shear strength<sup>11</sup> and accordingly concluded

<sup>11</sup>In Hamilton's paper, the shear strength refers only to cohesion.

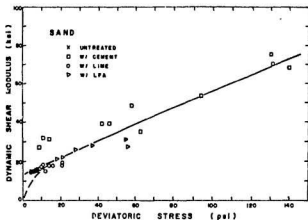


Figure 2.6: Dynamic Shear Modulus vs. Shear Strength(after Chae & Chiang, 1978)

that acoustical properties of unconsolidated deep-sea sediments were not a reliable indication of the shear strength.

#### 2.4.5 impedance vs. geotechnical properties

The acoustic impedance is defined as  $Z = \rho V$ , where  $V$  can be  $V_s$  or  $V_p$ . This property determines the amount of energy reflected when sound energy passes from one medium into another of different impedance. It is reported that density and porosity show almost perfect linear correlation to impedance. Impedance increases with density[87]. In-situ tests were carried out by Smith[88] who developed an equation as follows:

$$Z = 2.733 + 0.0014S - 0.721W_L \quad (2.27)$$

where  $S$  = vane shear strength;

$W_L$  = liquid limit.

It is very useful to note that the above equation relates acoustic impedance  $Z$  with shear strength although apparently it is only for cohesive soils. If a piezoelectric ceramic transducer is employed in acoustic testing, the electric impedance of the transducer can be concurrently measured and related to acoustic impedance [89, 90]. This method was only tried to distinguish between different sediments.

## 2.5 Discussion and Summation

As static and dynamic properties of soils are required for design purposes, a rough correlation between them is inevitable. One approach is to calculate dynamic properties from measured acoustic velocities and to correlate them, through laboratory experiments, to static properties at different strain levels. However, it is argued that the good agreement between the measured values could be fortuitous. The correlation technique certainly has merits as well as demerits. Owing to the paucity of detailed data, a critical assessment of the variation of shear wave velocity with shear strength is difficult to make. Yet, special attention should be paid to several subjects so that the nexus and difference between shear strength and acoustic properties could be understood fully in order to take advantage of the merits of the correlation technique.

### 2.5.1 Strain rate

Various reasons can be postulated for the disagreement between static and dynamic tests. To begin with, the strain rate is different in these tests. While trying to correlate acoustic properties with strength characteristics of a soil, we are really attempting (1) to relate static and dynamic moduli, and (2) to make use of a tacit assumption that shear wave velocity  $V_s$  is a usable measure of cohesion and internal friction. Usually,

static moduli are computed from stress-strain relationships under relatively a large range of strains. Dynamic moduli are calculated from the relationships of elastic stress waves as given by the equation  $G_{max} = \rho(V_s)^2$ . It is reported that, under the same test conditions, the dynamic moduli were considerably greater than the static moduli[91, 92] and the dependency of the dynamic modulus on the effective confining pressure was less than for the static modulus. Similar results were obtained by Schultheiss[56, 57] who conducted acoustic-oedometer tests and triaxial tests with acoustic benders. Hamilton[85] studied the cohesion and shear modulus of sediments and found that usually dynamic rigidity was about 4 orders of magnitude greater than cohesion. Seed and Idriss [52] stated that shear wave velocity was poorly related to undrained shear strength of clay because of the relative large variations in their results as shown by the ratio in the equation(2.21).

The disagreements mentioned above may be caused by the drainage conditions or strain rates considering that most of those results were from cohesive soils. Drainage is not accounted for in the elastic formulation  $G_{max} = \rho(V_s)^2$ . In the acoustic test, apart from measurements at very low frequencies, the modulus is determined under a very high strain rate; thus, there probably is insufficient time for either a change in the structural arrangement of the individual particles or accumulation of pore water pressure. In the static test, the strain rate is so slow that the soil has sufficient time to undergo changes in structure or to experience a pore water pressure increase. The combined effect of these factors is a larger deformation and, therefore, a smaller modulus in the static tests.

In spite of the anomalies, some researchers assert that it is still possible to make an assessment of strength magnitude from acoustic information [88]. The situation is different with cohesionless soils where there are no serious drainage problems. Whitman et al [93] found in their experiments that the static modulus of dry sand, measured using very small stress increments, roughly agreed with the dynamic modulus. Based on the experimental results from resonant column tests, Bolton and Wilson[94] also reported extremely good correlation between static and dynamic moduli for dry sands. They even concluded further that dynamic tests on dry sands may also be considered unnecessary. These favorable correlations may be because the hysteresis in dry sand is strain-rate independent, which is not true for cohesive materials.

### 2.5.2 Strain level

Another factor which could be responsible for the above difference is the different values of strain involved in the two different techniques. As far as its stress strain behavior is concerned, sand is by its nature nonlinear. When the strain level is low enough, a linear elastic model is of moderate precision, which is the case with respect to wave propagation. In the dynamic test, the strain is generally small enough to be considered in the pure elastic range. The highest shear modulus is obtained at lower shear strain levels. Therefore, the value deduced from acoustic measurements is relevant to elastic deformation. Basically, this stipulation has to be met as an essential condition as required by the equation(2.2). However, in the triaxial test, the strain extends beyond the pure elastic region resulting in a plastic shear deformation in soil.

From the above discussions we can see the pivotal point that to obtain the acoustic-

mechanical correlation for geotechnical applications it is essential to use a dynamic elastic model of soil to predict its static and dynamic plastic behavior. On the other hand, in the acoustic measurement the strain is the shear strain  $\gamma$  corresponding to the dynamic modulus  $G$ . Otherwise in the static triaxial test, the strain is the axial strain  $\epsilon$  corresponding to Young's modulus  $E$ . In the past decades, several experiments were conducted to study the effects of  $\gamma$  on  $G$ . As discussed before,  $\epsilon$  affects  $V_s$  as well. In the present research, the shear strain  $\gamma$  is kept small enough while  $\epsilon$  is increased until failure of the samples occurs.

### 2.5.3 In-situ and laboratory techniques

From equations (2.19) to (2.27) we can see that most of the previous correlations were made between in-situ undrained strength and acoustic velocity  $V_s$  or  $G_{max}$  for cohesive soils. It should be noted that the undrained shear strength  $S_u$  is influenced by the mode of failure and the rate of strain and therefore there is no unique value of the undrained shear strength [95, 96]. Unfortunately, our knowledge and skill in interpretation of in-situ undrained states are more limited. Usually, different types of in situ strength tests measure different values of  $S_u$  because those tests cause different modes of failure and strain rates [97, 99]. Wroth [98] suggested that specialized laboratory tests should continue to play an important role in determining strength parameters and the conventional triaxial compression test should be adopted for any comparisons or correlations.

With respect to the correlation between acoustic and mechanical properties of soils, the need to launch extensive laboratory-based investigations is more conspicuous than

ever before. The resonant column test can be designed to operated simultaneously with the triaxial test, but it is costly and complicated. It certainly can not be used in situ. Therefore, it is necessary to develop integrated techniques to model the prototype. The acoustic bender technique is one of those. The bender technique is more economical and convenient, and has been widely used now in laboratory testing[100, 101, 102]. The comparative studies prove that the shear strain amplitude from an acoustic bender transducer is of the order of  $10^{-6}$  and the measured shear moduli are quite close to that measured from resonant column testing.

#### 2.5.4 Summation

The correlations between  $V_s$  and major geotechnical strength properties are desirable since conventional methods of measuring soil strength can be affected by the fact that undisturbed samples are difficult to obtain for laboratory testing. From a review of the existing research results, it can be concluded that the correlation technique can be applied to sands with confidence but more laboratory studies and theoretical considerations are needed before extrapolating the laboratory results to in-situ applications. The acoustic bender method is a promising approach for the purpose of bridging laboratory tests and field methods. However, no successful breakthrough has yet been achieved in providing reasonable strength characterization through acoustic measurements. A complete understanding of the interrelationships between static and dynamic properties is still unavailable both empirically and theoretically. The correlations as discussed above remain to be perfected further. It is necessary to better understand their physical background, to develop new correlation models, and improve laboratory and in-situ testing methods.

## Chapter 3

# Equipments, Materials and Experimental Program

The part played by laboratory testing in the successful application of soil mechanics to civil engineering problems depends both on the uniformity of the natural strata and on the experience and skill of the engineer.

- Bishop & Henkel[103]

The objective of this research is to correlate shear strength with relevant acoustic properties of soil. Currently, our laboratory has only triaxial testing equipment, a direct shear machine and a miniature vane shear device that can be used to measure shear strength of soils. The triaxial device was chosen for the research. In order to measure soil shear strength and acoustic properties simultaneously, modifications were done on the existing triaxial cell. This chapter presents modifications and designs of all equipment employed in the experiments. The soils used in the program are also described in this chapter. The details of the test procedures are included in Appendix A. The technique of Hilbert transform was employed to estimate the propagation-time of shear wave travelling through the soil samples. This novel technique and instrumentation are presented separately in the following chapter.

## 3.1 Triaxial System

### 3.1.1 General Description

The triaxial loadframe used in this study is the Digital Tritest 50 from ELE International, England. This 50kN capacity machine comprises a rigid twin column construction with an integral fully variable microprocessor controlled drive unit. The machine is bench mounted for ease of installation and operation. All operating controls are mounted on the front panel of the machine. The machine is shown in figure(3.1). Originally, the crosshead position was difficult to be adjusted by moving four nuts on two columns up or down. Therefore, one slot was cut at one end of the crosshead so that it can swing on one column to easily accept a wide range of test apparatus.

The use of a microprocessor controlled drive system provides the Digital Tritest 50 with the following main advantages:

- single range fully variable speed control from 0.00001 to 5.99999 mm/min;
- speed set by direct reading digital switches;
- accuracy of platen speed  $\pm 1\%$  in either the unloaded or loaded condition; and
- self-check routine every time the machine is switched on.

The microprocessor and an RS232 port situated at the rear also enables the machine to be controlled remotely or to operate under external computer control, considerably enhancing its scope and performance. All functions of the load frame can be controlled through the RS232 interface including: speed, load and unload, and stop. Under these control conditions, typical geotechnical applications can be performed including:

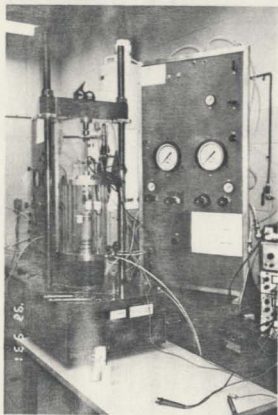


Figure 3.1: Digital Tritest 50 and Control Panel

constant rate of load, constant rate of stress, cyclic loading and stress path tests. Other features of the machine include: platen overtravel limit switches with flashing LED's to indicate travel limit, 25mm/min rapid approach/unloading speed and re-settable thermal overload to prevent drive system damage.

### 3.1.2 Triaxial Cell

The triaxial cell was manufactured at the Engineering Machine Shop of Memorial University of Newfoundland. Usually, the cell chamber is filled full of water and the load cell<sup>1</sup> is mounted outside the chamber along the loading ram. In this way, however, the frictional force between the loading ram and the teflon bushing will be included in load cell readings. The frictional force changes from time to time and is difficult to be offset by calibration. In order to overcome this shortcoming, a modification was introduced by moving the load cell into the triaxial chamber and adding a smaller inner cylinder for keeping water or other kind of liquids surrounding soil sample to deter air migration into the sample. A metal grid guard was put on the outer cylinder to prevent an explosion when the chamber pressure is high.

In the acoustic measurements, when frequencies are low, the geometric divergence effect may become important. As a rule, operations should be carried out at distances from the wave source such that the emitted wave is virtually a plane wave. The range of this working interval depends on the size of the bender element, the wavelength emitted, and the distance between the emission and observation points. Considering the possible reflection of shear wave by the membrane and the oscilloscope ability to

---

<sup>1</sup>Or load transducer.

measure the wave travelling time through the soil, the sample diameter was therefore enlarged to 50mm and the length to 100mm. On both top and base plates, there are several ports for transducer wires, air pressure, water and drainage. The whole assembly is shown in the figure(3.2).

### 3.1.3 Control Panel

All ports from the triaxial cell assembly, except some electrical ones, were connected by tubes to the control panel. Pressure transducers and gauges, volume transducer and valves are mounted on the control panel. The volume transducer was designed and manufactured at the Engineering Electronic Shop of Memorial University of Newfoundland. The calibrations of transducers are presented in Appendix A. These transducers are connected to the A/D board in the computer. A current-to-pneumatic transducer and a pressure amplifier are also installed on the control panel. This I/P transducer is connected to a D/A board in the computer and can provide a 3 to 15 psi output proportional to a DC milliamperre input from the computer controller. The arrangement of the control panel is illustrated in figure(3.3).

A closed control loop was then set up for the experimental operations. The computer program acquires data from the pressure transducers and LVDT and does real-time analyses to calculate stress, strain and pore pressure. These measurements are then compared with parameters preset in the program. According to these comparisons, signals are consequently sent out to I/P transducer and microprocessor in the Digital Tritest 50 loadframe. Through the combination of pressure flow by adjusting the control panel and the movement of the motor, we can do several different tests

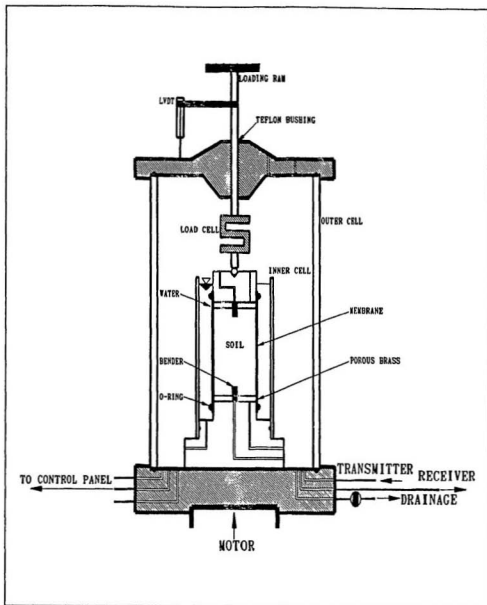


Figure 3.2: Triaxial Cell Assembly

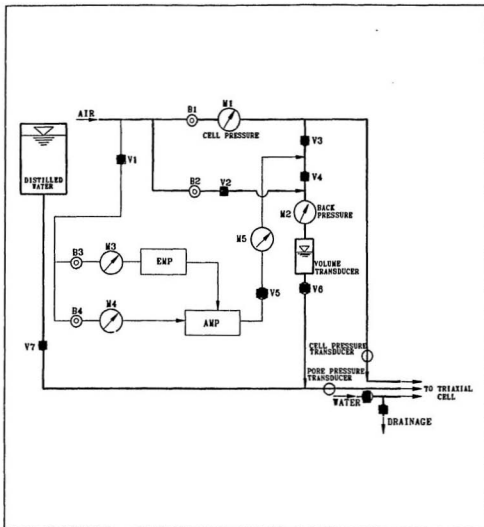


Figure 3.3: Flow Chart of Control Panel. In the figure, M1...M4 indicate pressure meters; B1...B4 indicate pressure regulators; V1...V7 indicate valves.

such as strain controlled, stress controlled, cyclic loading and stress path tests. The complete acoustic triaxial device assembly is shown in the Appendix A.

## **3.2 Hardware and Software for Data Acquisition and Control**

### **3.2.1 Hardware**

The data acquisition/control system used for the experimental program is made up of four main pieces of hardware. The largest part of the system is a 386SX-20MHz computer that is a high speed, highly integrated Intel's 80386SX microprocessor. The motherboard has a socket for 16/20MHz Intel 80387SX numerical coprocessor and a total of eight expansion slots, from which an advanced data acquisition and control system can be built.

Inside the computer, one MetraByte's DAS-8(analog to digital converter) board and one CIO-DDA06(digital to analog converter) board were installed on the mother board. The DAS-8 A/D board contains 8 analog input channels with 12bit resolution. The full scale input of each channel is  $\pm 5$  volts. Inputs are single ended with a common ground and can withstand a continuous overload of  $\pm 30$  volts. The CIO-DDA06 D/A board provides 6 channels of 12bit resolution analog output. It has five voltage output ranges from  $\pm 2.5V$  to  $\pm 10V$ .

External to the computer are one CIO mini-terminal and two MetraByte's universal expansion interface EXP-16 multiplexers which take input from the 16 channels on top

of each board. Each EXP-16 concentrates 16 differential analog input into one analog output to the DAS-8 board. Therefore, totally we can use 8 EXP-16 boards to have 128 differential analog inputs. The EXP-16 can also provide signal amplification, filtering and conditioning.

### **3.2.2 Software**

Although software is included with A/D and D/A boards, it is not very user-friendly. In this study, a low-cost but powerful software CONTROL EG was used. This software was specially programmed for data acquisition and control with compatible MetaByte products of DAS-8, CIO-DDA06 and EXP-16.

CONTROL EG is an extremely powerful menu driven automation software for PC based measurement and control systems. It combines the features of data loggers, programmable controllers and closed loop PID controllers in one easy to use integrated package. CONTROL EG requires no programming. Complex formulas can be entered in simple algebraic notations. All options are immediately accessible through single keystrokes. The user can alternate between seven real-time displays while the system is collecting data. CONTROL EG can output data to a printer or to a disk file. These data can be subsequently input into popular analysis programs such as Lotus 1-2-3<sup>TM</sup>. The entire data acquisition and control system is shown in figure(3.4).

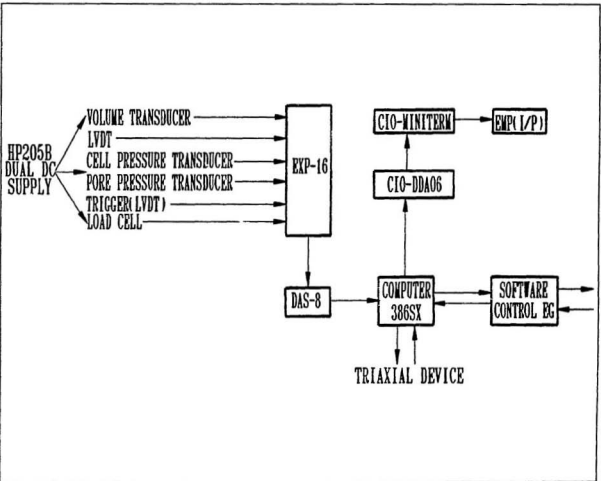


Figure 3.4: Layout of Data Acquisition/Control System

## **3.3 Acoustic Measurement Equipment**

### **3.3.1 General Description**

The central acoustic elements used in the research are piezoelectric ceramic benders. A piezoelectric substance possesses a useful combination of electrical and mechanical properties. The piezoelectrical phenomenon was discovered by Pieere and Jacques Curie in the 1880's[104]. Piezoelectricity is a property of certain classes of crystalline materials. When an electric field is applied to one of these materials, the crystalline structure changes shape, producing dimensional changes in the material. Conversely, when mechanical pressure is applied to one of these materials, the crystalline structure produces a voltage proportional to the pressure. These materials are used as electromechanical transducers.

Piezoelectric properties occur naturally in some crystalline materials and can be induced in other polycrystalline materials. Many contemporary applications of piezoelectricity use polycrystalline ceramics instead of natural piezoelectric crystals[105]. These piezoelectric ceramics are more versatile. Their physical, chemical, and piezoelectric characteristics can be tailored to specific applications. The hard, dense ceramics can be manufactured in almost any given shape or size. The ceramic bender element was first employed for geotechnical measurement by Shirley et al in 1977[90, 106, 107]. So far it has been widely used in geotechnical laboratories because of the advantages pointed out in the first chapter.

There are two different types of piezoceramic benders because of the different elec-

trical connection of two plates: one is connected in series with the polarization of the ceramics oriented in opposite directions for each plate, and the other one is connected in parallel in which the polarization of the ceramics is in the same direction for both plates. An applied voltage generates a greater bend in a parallel connected element, when used as a transmitter or generator of shear waves (electrical to mechanical energy). A series connected element generates a higher voltage when bent, which is used as a shear wave receiver or generator of electrical signals (mechanical to electrical energy).

In this research, the piezoelectric ceramic bimorph BM500 manufactured by Sensor Technology Limited was used. The bimorph is a double plate ceramic bender element. Two plates are bonded together so that they amplify their piezoelectric actions. The bender element dimensions are  $15 \times 10 \times 0.5$  mm. BM500 series ceramics are lead zirconate titanates with a high coupling coefficient and piezoelectric charge coefficient.

### **3.3.2 Installation of the Benders in the Triaxial Cell**

The bender element is a high impedance device that cannot be exposed to moisture as this could electrically short the transducer. A layer of epoxy was therefore coated around the element before it was mounted in the slots on the pedestal and cap in the triaxial cell. Epoxy was also used to fix benders in the slots. The porous brass disc with a corresponding slot was glued with epoxy to the pedestal and top cap. A piece of thin rubber was put between the bender and brass disc so that no part of the hard brass was in contact with the bender to prevent movement. The bender elements protrude about 10 mm long into a soil specimen. The longest dimension aligns with the longitudinal axis of the soil specimen. Figure(3.5) shows the mounted soil sample

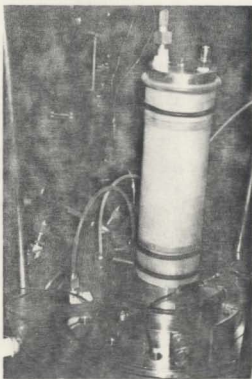


Figure 3.5: Soil Sample with Bender Elements at Bottom and Cap

with bender elements at the bottom and cap. The wire leads to the transducer are run through holes in the pedestal and cap and exit the cell through pressure-proof fittings in the cell base and top. The detail installation of bender elements is shown in figure(3.6).

When the bender is mounted, it protrudes into the specimen as a cantilever and causes a shear stress to develop when voltage is applied. Soil particles surrounding of the bender move in the same direction as the tip of the element. This will result in shear waves which propagate through the specimen in a direction parallel to the length of the relaxed element. In the triaxial cell, the shear wave transmits upwards. The shear wave will be detected in a reciprocal manner by the receiver bender element that is connected with the oscilloscope. The relatively large displacements which can be obtained for small applied voltages, coupled with the low resonant frequencies, make bender elements quite suitable as shear wave transducers for experiments within a triaxial cell.

### **3.3.3 Measurement of Shear Wave Velocity**

Due to the very short propagation time of the shear wave through the soil sample, a scope of high resolution and accuracy is needed to record the wave history. A Tektronix 2211 oscilloscope was used in this study. The Tektronix 2211 is a combination analog and digital storage portable oscilloscope. The resolution is 12bits. It has dual vertical input channels with an analog bandwidth of DC to 50MHz, a digital bandwidth of DC to 1MHz, and a CRT readout and cursor measurement display. The cursor display makes it extremely convenient and accurate to determine time-difference between the

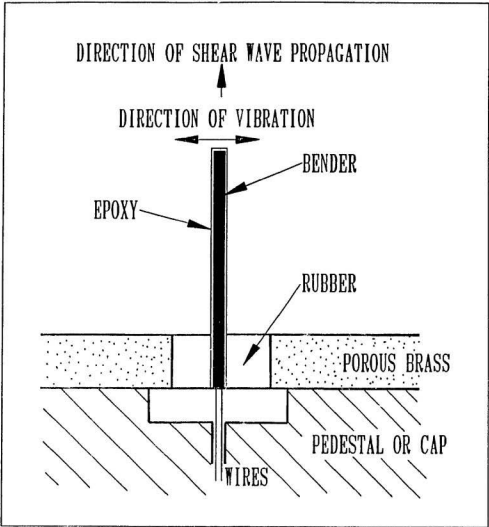


Figure 3.6: Installation of Bender Element

positions of the cursors on the displayed waveforms. The recorded waveform can also be plotted out using a plotter. Figure(3.7) sketches the connections. All the electronic equipments used in the experiment are shown in figure(3.8) .

A square wave with a frequency of 5 to 100 Hz was used to generate a shear wave. The signal from the receiver bender was monitored by the oscilloscope from which the traveling time was taken by using cursors between the rise of the trigger signal and the first arrival of the receiver signal. Figure(3.9) shows a picture of the typical waveform and travelling time recorded on the oscilloscope. It is assumed that the shear wave travels from the tip of the transmitter to the tip of the receiver. Let  $L$  be the tip-to-tip length of soil sample and  $T$  the propagation time. The shear wave velocity and corresponding shear modulus can be determined as follows:

$$V_s = \frac{L}{T} \quad (3.1)$$

In our experiment, the average travelling distance<sup>2</sup>  $L=73\text{mm}$ .

During each test, a LVDT was used to hit the external trigger button on the oscilloscope front panel. Every strike will trigger the oscilloscope to record a new waveform on its screen. At the same time, the displacement of the LVDT will be recorded by the computer together with other data from the triaxial shearing test. Those data were logged into the same data file from which we can locate the acoustic measurement and the corresponding shear strain at that specific point. This procedure allows us to calculate the shear wave velocity and the corresponding strain and deviator stress

---

<sup>2</sup> $L = L_s - 2l$ , where  $L_s$  is the sample height. Particular value of  $L$  in each tests may be different from 73mm. It depends on each measurement of  $L_s$ .

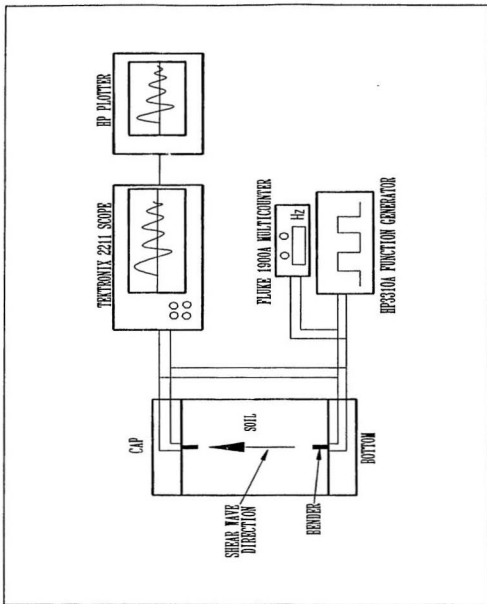


Figure 3.7: Setup for Acoustic Measurement in Triaxial Test



Figure 3.8: Electronic Equipment Used in the Acoustic-triaxial Test

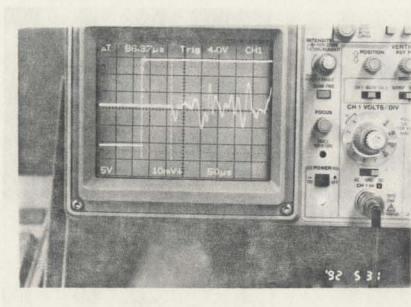


Figure 3.9: Record of Traveling Time and Shear Wave Received with an Oscilloscope

while the soil sample is being sheared. Therefore, we can compare shear wave velocity and shear strength on the same strain scale to study their relationship.

### 3.3.4 Discussion

With respect to the above measurements, difficulty arises in determining accurately the first shear wave arrival. Although the bender element presumably generates shear wave, compressional waves are very likely present as well. The receiver bender is very sensitive to the mechanical movement. A small vibration will generate a detectable electrical signal. On the other hand, the instruments employed in the experiment will affect in some way the excitation signal and the received signal. Actually, the received signal is a combination of shear and compressional waves, waves reflected by membrane, instrument noise and even the noise from the crushing and shearing of soil particles. Therefore, it is very difficult and arbitrary to determine the first arrival of shear wave form.

This problem may be overcome by changing the direction of the particle vibration so that the shear wave reverses polarity but the compression wave polarity remains the same as shown in figure(3.10). Dyvik and Madhus[108] used the reversed polarity property of shear wave to check the first shear wave arrival and concluded that the receiver element was monitoring only shear waves. However, by the author's experience , it is difficult in acoustic triaxial experiments to obtain exact mirror images of two shear waves in the opposite directions. Actually, Dyvik and Madhus's trace curves before the arrival of the shear wave. The curved trace makes it fuzzy to identify the point of the first arrival of the shear wave. As shown in figure(3.11), the received

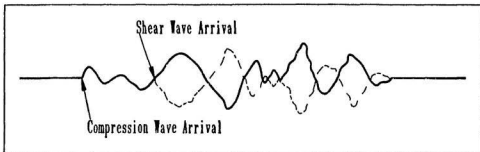


Figure 3.10: Polarity of Shear Wave Arrival

signal was recorded with test DT363 just before the sample was sheared. If the signal was a pure shear wave, then the measured travelling time should be  $\Delta T = 190.00\mu\text{s}$ . From equation(3.1) we can obtain the shear wave velocity  $V_{s1}=384.21\text{m/s}$ . This value is obviously greater than the reasonable one. As a comparison, using Hardin-Richart equation(2.12), we can obtain an estimated value  $V_{s2}=342.31\text{m/s}$ . The difference is about 13% between them. In the next chapter, the Hilbert transform will be introduced as a means to overcome these difficulties.

### 3.4 Materials Tested

In total, five sands were used. All are standard silica sands with different index properties as shown in table(3.1). Following ASTM D854<sup>3</sup>, the specific gravity was obtained at the temperature  $20^{\circ}\text{C}$ . The maximum and minimum void ratios were

<sup>3</sup>Refer to Annual Book of American Society for Testing and Materials, Vol.04.06.

$\Delta T$  0.1900ms Trig 5.0V CH1

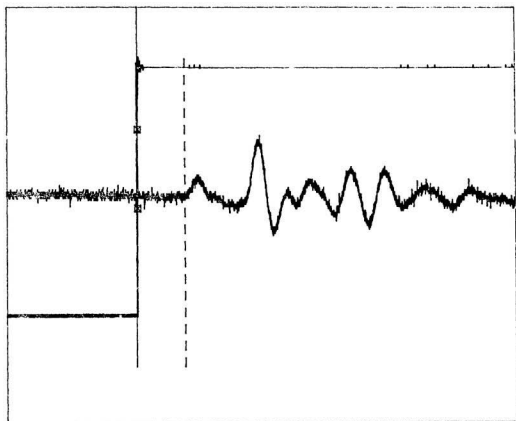


Figure 3.11: Typical Waveform(DT363) Recorded by Plotter

Table 3.1: Index Properties of Soils Tested

Sand 1: silica sand #0

Sand 2: Ottawa sand, ASTM 20-30 mesh

Sand 3: Ottawa sand, CN-501

Sand 4: silica sand #1

Sand 5: Cube test sand, ASTM C-109

Soil Type	$D_{60}(\text{mm})$	$D_{10}(\text{mm})$	$C_u$	$C_c$	$G_s$	$e_{min}$	$e_{max}$
Sand 1	1.00	0.65	1.54	1.33	2.65	0.65	0.83
Sand 2	0.78	0.69	1.13	1.43	2.65	0.49	0.62
Sand 3	0.86	0.45	1.51	1.51	2.65	0.50	0.65
Sand 4	0.50	0.32	1.56	2.67	2.65	0.68	0.94
Sand 5	0.36	0.24	1.50	1.19	2.65	0.51	0.74

measured using the procedures outlined in ASTM D4253 and D4254. Figure(3.12) shows the grain size distribution curves. The curves and classification were obtained from standard sieve tests(ASTM D421, D422 and D2487). From the distribution curves we can see that the sand particle sizes are quite uniform with no big difference among five sands. Therefore, similar mechanical behavior should be expected for each sand.

### 3.5 Experimental Program

Strain rate is not too important for dry sands. The motor speed was fixed at 1mm/min which corresponds to an axial strain rate of 1.08%/min. The relative density and stress state are two major factors which would affect the shear strength and shear wave velocity of sands. Because the sands are uniform, high density samples are difficult to achieve. On the other hand, a low density will influence the bender behavior because of the poor coupling between the acoustic bender and the soil particles. Four relative densities, i.e., 50%, 60%, 70% and 80% were used during the experiments to cope with these problems. Considering the capacity of transducers and electronic measuring equipment, confining pressures were selected ranging from 50KPa to 300KPa. All of these combinations are summarized in table(3.2).

Testing of homogeneous samples under uniform states of stress and strain is required for fundamental studies of soil property characterization. As mentioned in the last chapter, the sample preparation method will also affect soil behavior because various preparation method would cause different soil structures. Theoretical analysis and experimental evidence[109] suggests that reconstitution by pluviation is the most promising technique for obtaining uniform samples in the laboratory and allows

a convenient study of mechanical response of natural sands. In this research, an air pluviation technique was used to prepare the samples for testing. Additional vibration by tapping the side of mold was also necessary to densify air-pluviated samples to achieve the required relative density.

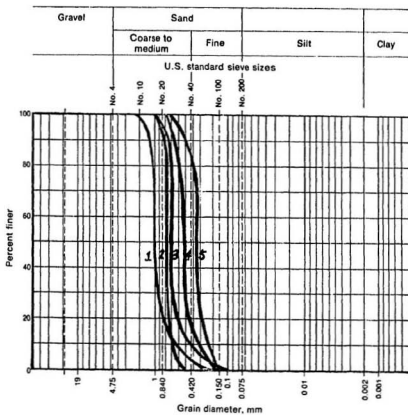


Figure 3.12: Particle Size Distribution Curves of the Soils Tested

Table 3.2: Acoustic Triaxial Test Program

		Sand 1	Sand 2	Sand 3	Sand 4	Sand 5
Axial Strain Rate		1.08(%/min)				
$D_r$ (%)	medium	50 60				
	dense	70 80				
confining pressure $\sigma_3$ (KPa)		50				
		100				
		200				
		300				

Table 3.3: Porosity and  $W_s$  Used in the Test Program

$D_r(\%)$		50	60	70	80
Sand 1	n(%)	42.53	41.93	41.31	40.69
	e	0.740	0.722	0.704	0.686
	$W_s(g)$	281.10	284.03	287.03	290.10
Sand 2	n(%)	35.69	35.15	34.60	34.04
	e	0.555	0.542	0.529	0.516
	$W_s(g)$	314.54	317.19	319.89	322.63
Sand 3	n(%)	36.51	35.90	35.28	34.64
	e	0.575	0.560	0.545	0.530
	$W_s(g)$	310.54	313.53	316.57	319.68
Sand 4	n(%)	44.75	43.95	43.12	42.26
	e	0.810	0.784	0.758	0.732
	$W_s(g)$	270.22	274.16	278.22	282.39
Sand 5	n(%)	38.46	37.58	36.67	35.73
	e	0.625	0.602	0.579	0.556
	$W_s(g)$	300.99	305.31	309.76	314.34

## NOTES

void ratio  $e = c_{max} - D_r(c_{max} - c_{min})$

porosity  $n = \frac{e}{1+e}$

for dry sand, solid particles weight  $W_s = \frac{\rho_s v}{1+e} \gamma_w$

unit weight of water  $\gamma_w = 1g/cm^3$

sample volume  $v = \pi r^2 L_o$

sample radius  $r=25mm$

sample height  $L_o=94mm$

## Chapter 4

# Hilbert Transform and Propagation-time Estimation

When you can measure what you are speaking about, and express it in numbers, you know something about it; but when you cannot measure it, when you cannot express it in numbers, your knowledge is of a meager and unsatisfactory kind; it may be the beginning of knowledge, but you have scarcely, in your thoughts, advanced to the stage of science.

- William Thomson(Lord Kelvin)

### 4.1 Introduction

The precise calculation of shear wave velocity depends on the accurate estimation of shear wave travelling time through the sample. Chapter 3 included a description of the method used with the digital storage oscilloscope to measure time delay between the triggering signal and received signal. As discussed before, this approach faces a major difficulty, i.e., identification of the shear wave front or the first arrival of a shear wave. The calculation shows about 13% difference between the measured value and the estimated value from equation(2.12). This problem may be improved by the Hilbert transform.

Transformations of data from one form to another are common in signal analysis, and various techniques are used to extract significant information from time series. Interpreting data from different points of view often results in new insight and the discovery of relationships not otherwise evident. The conventional acoustic trace can be viewed as the real component of a complex trace which can be uniquely calculated under usual conditions[110]. The complex trace permits the unique separation of envelope amplitude and phase information and the calculation of instantaneous frequency. Expressing acoustic data in complex form also yields computational advantages.

In virtually all types of experiments in which a response is analyzed as a function of frequency or time, transform techniques can significantly improve data acquisition and/or data reduction. The Hilbert transform is one of the techniques. Particularly, the Hilbert transform detects hidden signals. It has a variety of applications; the one to be mentioned here concerns solving the problem of determining wave propagation-time. By means of Hilbert transform, the envelope of a time signal can be calculated and the estimation of propagation time can be obtained. Such a transform technique offers at least two main advantages for acoustic signal processing. First, the transform provides a variety of simple procedures for manipulating digitized data, such as smoothing or filtering to enhance signal-to-noise ratio and resolution enhancement. Second, the transform technique can be used to move any known irregularities in the excitation waveform, so that the corrected response reflects only the properties of the sample, and not the effect of the measuring instrument. Oscilloscopes use the raw source of signals in an analog way, but the Hilbert transform technique processes the signal first then extracts information from the treated data in a digitalized way. With the

Hilbert transform technique, it is not necessary to pinpoint the first arrival of shear wave and hence it is possible to eliminate the arbitrariness and external influence in the determination of shear wave travelling time.

## 4.2 Hilbert Transform

The Hilbert transform is a method of separating signals based on phase selectivity, which uses phase shifts between the pertinent signals to achieve the desired separation. When the phase angles of all components of a given signal wave are shifted by  $\pm 90^\circ$ , the resulting function of time is known as the Hilbert transform of the signal. Unlike the Fourier transform  $X(f)$  which moves the independent variable of a signal  $X(t)$  from the time domain to the frequency domain, the Hilbert transform leaves the signal  $X(t)$  in the same domain. The Hilbert transform  $\hat{X}(t)$  of a real-valued time signal  $X(t)$  is another real-valued time signal, and the Hilbert transform  $\hat{X}(f)$  of a complex-valued frequency function  $X(f)$  is another complex-valued frequency function.

There are three different ways to define the Hilbert transform. The easy and useful one is to introduce an analytic signal  $Z(t)$  to compute the Hilbert transform  $\hat{X}(t)$  of the given signal  $X(t)$  as follows[111]:

$$Z(t) = X(t) + j \hat{X}(t) \quad (4.1)$$

where  $j = \sqrt{-1}$ . This equation can also be written as

$$Z(t) = V(t) e^{j\phi(t)} \quad (4.2)$$

The Hilbert transform  $\hat{X}(t)$  is the imaginary part of  $Z(t)$ , i.e.,

$$\hat{X}(t) = \mathcal{H}[X(t)] = \Im[Z(t)] \quad (4.3)$$

where  $V(t)$  is called the instantaneous amplitude or envelope signal and  $\phi(t)$  is called the instantaneous phase signal:

$$V(t) = \sqrt{X^2(t) + \dot{X}^2(t)} \quad (4.4)$$

and

$$\phi(t) = \tan^{-1} \left[ \frac{\dot{X}(t)}{X(t)} \right] \quad (4.5)$$

Acoustic measurements results in a time signal containing a rapidly oscillating component. By using the Hilbert transform, the rapid oscillations can be removed from the signal to produce a direct representation of the envelope alone, which allows detailed study of the envelope. The envelope often contains important information about the given signal. The envelope has another advantage. Since  $V(t)$  is a positive function, it can be graphically represented using a logarithmic amplitude scale to enable a display range of 1:10000 or more. The original signal  $X(t)$  includes both positive and negative values and limits the display range to about 1:100.

The propagation time from point  $X$  to point  $Y$  of a signal is usually estimated by measuring the signal  $X(t)$  at  $X$  and the signal  $Y(t)$  at  $Y$ , and calculating the cross-correlation function  $R_{xy}(t)$ . Like the autocorrelation function, the cross-correlation function provides a measure of the similarity between a signal and the time-delayed version of a second signal:

$$R_{xy} = E[X(t)Y(t + \tau)] = \lim_{T \rightarrow \infty} \frac{1}{2T} \int_{-T}^T X(t)Y(t + \tau) dt \quad (4.6)$$

where  $E[ \ ]$  is the expected value of the item within the brackets. From the cross-correlation function, we can obtain the signal travelling time as shown in figure(4.1).

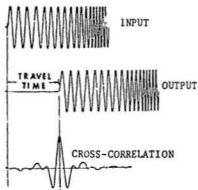


Figure 4.1: Cross-correlation to Find Travel Time

However, cross-correlation function includes all values in the range  $(-\infty, \infty)$ . The positive and negative peaks or, most of time, none of them could indicate the propagation time. Instead, by using the Hilbert transform, the correct propagation time can be easily and solely found from the envelope of the cross-correlation function  $R_{xy}(t)$ , whether or not the peak of  $R_{xy}(t)$  corresponds to the travel time. The maximum of the envelope always indicates the correct wave propagation time. This is the principle used in the experiments to determine propagation time of shear wave travelling from the bottom to the top of the soil sample in the triaxial cell.

### 4.3 Instrumentation and Data Analysis

The equipment used for recording signals is multichannel waveform recorder DATA-LAB DL1200 at C-CORE of Memorial University of Newfoundland. The DL1200 is a

digital instrument designed to acquire multi-channel analogue signals. An IEEE-488 interface board was plugged into 386SX computer so that the Datalab recorder was connected to the computer through a GPIB interface cable.

The software for acquiring signals and performing the Hilbert transform was also developed at C-CORE. After Datalab captures the time series of wave form and plots it on the screen, the program can further carry out Hilbert transformation of the signal and plots its envelope below the original wave form. All the data can be converted into HPG files which can be put into a Wordperfect file for printing.

As a comparison, under the same soil sample conditions of DT363 as shown in figure(3.11), the test was repeated with DATALAB recorder. Figure(4.2) shows the record of the original time signal and the corresponding envelope by Hilbert transform obtained by DATALAB software. From the figure of the envelope we can find the correct propagation time  $\Delta T = 212\mu s$ . We can see that this value is not equal to the one in time series corresponding to the peak of the signal, nor does it equal to the value obtained in figure(3.11). From the envelope measurement and the equation(3.1), the shear wave velocity can be obtained  $V_{s1} = 344.34\mu s$  that is very close to that from Hardin-Richart equation(2.12) where  $V_{s2} = 342.31\mu s$ . The difference between them is only 0.59%. Referring to the results in the Section(3.3.4), we can see that the Hilbert transform technique is much better than using an oscilloscope.

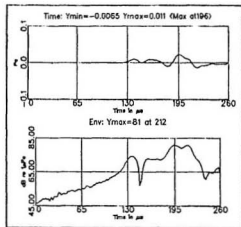


Figure 4.2: Propagation Time Estimated by Hilbert Transform. The envelope curve indicates propagation time  $\Delta T = 212\mu s$ .

## Chapter 5

# Experiment Results and Analyses

Scientific understanding proceeds by way of constructing and analysing models of the segments or aspects of reality under study. The purpose of these models is not to give a mirror image of reality, not to include all its elements in their exact sizes and proportions, but rather to single out and make available for intensive investigation those elements which are decisive. We abstract from non-essentials, we bolt out the unimportant to get an unobstructed view of the important, we magnify in order to improve the range and accuracy of our observation. A model is, and must be, unrealistic in the sense in which the word is most commonly used. Nevertheless, and in a sense, paradoxically, if it is a good model it provides the key to understanding reality.

- Baran & Sweczy[112]

The demand for more reliable methods of predicting the stress-strain relationship of marine sediments makes it very important to develop a reliable model to accurately evaluate the behavior of soils under various loading conditions. Loose sand and dense sand behave differently in the triaxial tests. The following hyperbolic model is usually applied in the case of loose sand:

$$\sigma = \frac{\varepsilon}{a + b\varepsilon} \quad (5.1)$$

But for dense sand, up to now there is no concise model. This chapter presents a new

model whereby the shear strength of sand can be compared and studied based on their behavior during shear. Following the establishment of the stress-strain relationship, the acoustic properties of the sand are studied. The shear strength and shear wave velocity are correlated using the new constitutive equation. As foregoing chapters have shown, the correlations between static and dynamic test data are variable and the few mechanisms involved are mostly subject to considerable debate. Therefore, in this chapter, the experimental results are first presented in each section, and then, the data are interpreted to understand the causes behind the physical phenomena.

## 5.1 Stress-Strain Relationship

In the triaxial test, confining pressure and relative density are two primary effects controlling the shear behavior of sands. As shown in figure(5.1), three samples of sand #5 with the same relative density were sheared respectively under three confining pressures. The higher the confining pressure, the stiffer the sample and hence the higher the shear strength. In order to find the value of internal friction angle  $\phi$ , the test data were plotted again in the  $p_f$  vs.  $q_f$  figure. It can be seen in the figure(5.1) that three  $q_f$  points on stress paths are very close to the average  $K_f$  line. These results demonstrate that the new triaxial testing system, including the main frame, modified triaxial cell, all transducers and data acquisition/control software, works fairly well and can provide excellent measurements. The experimental data were also analyzed by constructing Mohr circles and drawing Mohr envelope. Other experimental results are included in Appendix B.

For granular sand, the shear resistance is considered as having several attributes.

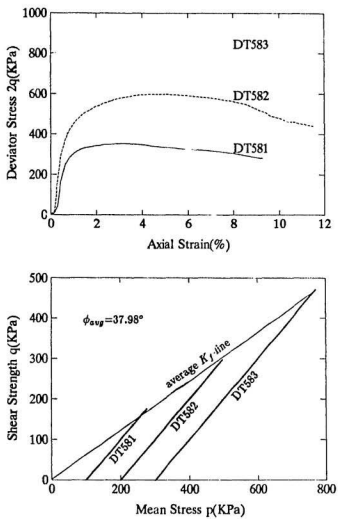


Figure 5.1: Effect of Confining Pressure on Strength

The major one is the resistance against relative particle movement or reorientation. Therefore, relative density and particle size distribution should have effects on the strength of sand. Usually, the denser soil has higher strength due to more interlockings among soil particles, which is shown in figure(5.2). Yet the effect of relative density is not as notable as that of confining pressure. In figure(5.3), we can see that the deviator stress of the coarser sand(DT182) is greater than that of the finer sand(DT582). From a qualitative viewpoint, it is probable that mutual displacement among coarse particles is more difficult to occur because a sand particle must use more energy to move over a bigger one.

From foregoing figures we can observe that, for soil samples with relative densities from 50 to 80 per cent, the deviator stresses increase with increasing axial strain to the maximum values, then decrease with axial strain. After examined the results from about forty triaxial tests on sands, the author found that the stress-strain behavior of sands with relative density from medium to dense could be described using the following equation:

$$\left(\frac{\sigma_1}{\sigma_3} - 1\right)^{1-n} = (1 + d\varepsilon)^{\frac{c}{a+br}} \frac{\varepsilon}{a + b\varepsilon} \quad (5.2)$$

where  $n$ ,  $a$ ,  $b$ ,  $c$  and  $d$  are parameters that can be determined from experiments. In the equation, stress ratio  $\frac{\sigma_1}{\sigma_3}$  is used so that all parameters are dimensionless. In addition, in this research, for each soil sample, confining pressure  $\sigma_3$  is kept unchanged. Therefore, equation(5.2) can be rewritten in the following form for the purpose of convenience in processing the data:

$$(\sigma_1 - \sigma_3)^{1-n} = \sigma_3^{1-n} (1 + d\varepsilon)^{\frac{c}{a+br}} \frac{\varepsilon}{a + b\varepsilon} \quad (5.3)$$

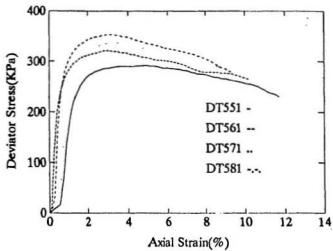


Figure 5.2: Effect of Relative Density on Strength

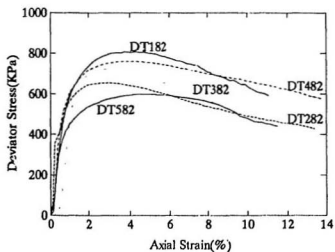


Figure 5.3: Effect of Grain Size on Strength

It is noted that equation(5.2) becomes a hyperbolic equation when  $c = 0$ , which is shown in figure(5.4). When very large axial strain occurs, both equation(5.2) and the hyperbolic equation will take asymptotically the same value of ultimate strength  $(\sigma_1 - \sigma_3)_{ult}$ . Virtually, the equation(5.2) can be applied to soils with a wide range of relative densities from loose to dense. Figure(5.4) also shows the measured data with the test DT262. It is seen that with properly chosen parameters, the above equations can model well the measured stress-strain curve. With the same parameters obtained in the test DT262, the equation was used to fit the results from tests DT583, DT582 and DT581. Comparisons are shown in figure(5.5) in which we can see that, for each test, the curves from model calculations can fit the measured ones. Especially the data from the model are very close to the measured values when the sample is about to reach its maximum strength and after the failure. However, discrepancies exist before the failures occur. The difference between the model and the test data is more remarkable for the test DT582.

From the examinations on all experimental results, it is found that the parameters  $b$ ,  $c$  and  $d$  in the model remain almost unchanged with different sand type, relative density and confining pressure. Because of the transcendental property in equation(5.2), the usual regression methods are not suitable to obtain parameters in the equation. Therefore, optimal parameter identification technique is used. For each parameter, an initial value is given. The calculated values are then compared with the measured ones. Based on the comparison, the second value is further chosen for each parameter. After several iterated interpolations, optimal parameters can be finally obtained. In this study, the following values were used:

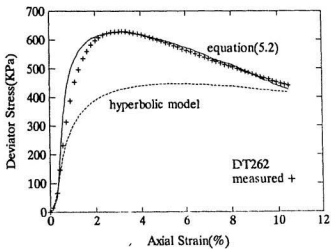


Figure 5.4: Test Data(DT262) and Modelling Curves

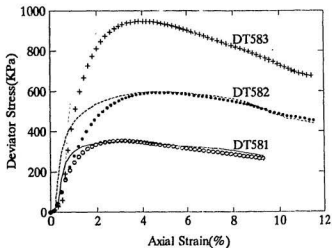


Figure 5.5: Comparison of Model and Test Data( $D_r = 80\%$ )

$$b=1.2$$

$$c=0.0067$$

$$d=35.5$$

However, the parameters  $a$  and  $n$  change slightly with different conditions.  $a$  varies from 0.0013 to 0.002 and  $n$  varies from 1.07 to 1.1. It is further found that  $a$  relates to the axial strain magnitude and  $n$  to the confining pressure magnitude. More comparisons between the model and the test data are shown in figure(5.6) and also in the Appendix B.

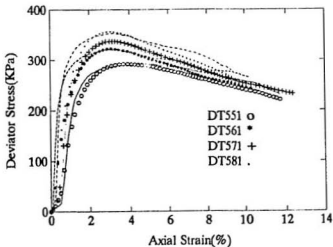


Figure 5.6: Comparison of Model and Test Data( $\sigma_3=100\text{KPa}$ )

## 5.2 Acoustic Experiments

Various factors exert influences on the shear wave velocity in the soil. Among them are confining pressure, void ratio, amplitude of strain, degree of saturation, soil fabric, stress strain history, and so forth. It has been shown that for lower shearing-strain amplitudes, shear wave velocity is essentially independent of each of these variables except for confining pressure and void ratio. This can be expressed in the following form:

$$V_s = f(\sigma_o, e) \quad (5.4)$$

in which  $\sigma_o$  is average effective confining pressure and  $e$  is void ratio. The frequency of the acoustic signal has only a minor effect on the measured shear wave velocity in this study. The following table indicates small increases in velocities with increasing signal frequency. But when the frequency is too high, the measured travelling time is not correct due to the limitation of the equipment used. Therefore, the frequency of about 5Hz was used in this study.

Table 5.1: Effect of Signal Frequency

Test DT46						
Hz	5	15	20	50	80	100
$V_s$	201.66	201.01	200.89	202.24	205.89	210.96

In the acoustic experiments, two different tests were conducted. One was carried out to measure the shear wave velocity before the soil sample was vertically sheared. The other one was carried out after starting shearing soil sample. To begin with, before the shearing, acoustic measurements were taken from the sample under the confining

pressure. It was found that, for all kind of sands used in the tests, the shear wave velocity decreases linearly with increasing void ratio, which is shown in figure(5.7). Figure(5.7) also illustrates clearly the significant effect the confining pressure has on the shear wave velocity of sands. In detail, it is observed that the shear wave velocity increases nonlinearly with increasing confining pressure. The curve was fitted through the test points corresponding to the different confining pressures. For each set of tests with different types of sands, the effect of confining pressure on shear wave velocity is shown to be significant. From regression analyses, the following equation was obtained:

$$(V_s)_0 = (19.76 - 8.68e)\sigma_v^{0.25} \quad (5.5)$$

where  $(V_s)_0$  is the shear wave velocity corresponding to the zero axial strain. The wave velocity from this equation have consistently been found to agree with those obtained in the tests. The error ranges are indicated in figure(5.7) using the vertical bars. With confining pressure at 300KPa, the error range of shear wave velocity is within  $\pm 5\%$ . However, when confining pressure is lower, for instance, 50KPa, the error range of shear wave velocity could be as wide as  $\pm 20\%$ . This is because at low confining pressure, the coupling between soil particles and bender elements is poor, which causes errors in the acoustic measurements. However, from equation(5.5), the maximum variation of shear wave velocity with change of void ratio may still be evaluated for any sand by considering the values of velocity corresponding to the maximum and minimum void ratios and a given confining pressure. These values will bracket the correct value for shear wave velocity for this sand in-situ subjected to this same value of confining pressure.

When a vertical stress is applied to shear the sample, the acoustic characteristics

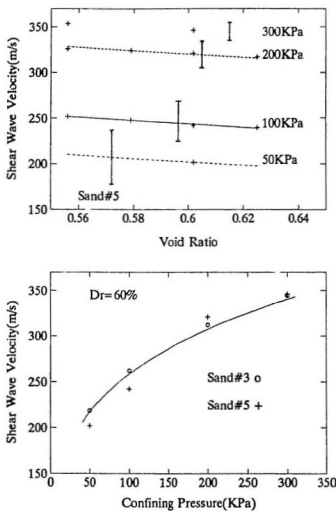


Figure 5.7: Effect of Void Ratio and Confining Pressure on Velocity

of the soil will be different in some ways. The above equation can not closely match the measured values. As discussed in Chapter 2, while large axial strain occurs, soil structure changes, for instance, due to particle reorientation. When this happens, the shear wave velocity is no longer independent of the strain and soil structure. If shear wave velocity is plotted versus axial strain as shown in figure(5.8), it can be found that during the first stage of shearing, the shear wave velocity increases with increasing axial strain. After reaching its maximum value, the velocity varies slightly for a while although axial strain still increases. However, when axial strain develops further, the shear wave velocity drops slowly. The rate of decreasing in shear wave velocity depends on the type of soil and the magnitude of confining pressure. In figure(5.8), it can also be seen that, in every case, an increase in velocity occurs with increasing effective pressure, but this increase depends substantially on the type of soil concerned, which will be discussed in the following paragraphs.

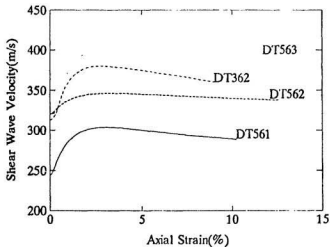


Figure 5.8: Effect of Axial Strain and Confining Pressure on Shear Wave Velocity

It should be noted that the relative density of the material has a negligible influence on the shear wave development with axial strain. If we examine the wave velocities normalized with  $(V_s)_0$ , shown in figure(5.9), it can be seen that they are quite close for the tests DT352, DT362 and DT382, even though the relative densities for the three samples are 50, 60 and 80 per cent respectively. In each case, only a slight increase in velocity occurs with increasing relative density for the same type of material. However, for a different type of sand, the shear wave velocity may change substantially. For example, in figure(5.9), the shear wave velocity of DT362 is much higher than that of DT562. Both samples are of 60 per cent relative density and under the same confining pressure  $\sigma_3 = 200\text{KPa}$ , but are two different sands. According to the analysis in the Section(5.1) that, under the same confining pressure, coarser sand has higher rigidity than finer sand does, the phenomenon shown in the figure(5.9) is ready to be understood. Referring to the particle size distribution curves in the figure(3.12), it is seen that the particle size of sand#3 is bigger than the particle size of sand#5. More specifically in the table(3.1), we can find that for sand#3,  $D_{60}=0.86\text{mm}$ ,  $D_{10}=0.45\text{mm}$ , and for sand#5,  $D_{60}=0.36\text{mm}$ ,  $D_{10}=0.21\text{mm}$ . Averagely, the particle diameter of sand#5 is only the half size of sand#3.

If we carefully observe figure(5.9) and figure(5.1), it is inevitable to take notice of the similarity between the stress-strain relationship and the velocity-strain relationship. For the convenience of comparison, it is helpful to put them in the same figure as shown in figure(5.10). Like the deviator stress, shear wave velocity increases with axial strain during shear. Velocity reaches its maximum value approximately when the deviator stress no longer increases. The maximum values of both deviator stress and shear wave

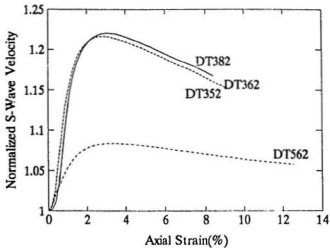


Figure 5.9: Effect of Relative Density and Type of Sands on Shear Wave Velocity

velocity correspond approximately to the axial strain at failure. With test DT561, the shear wave velocity drops immediately after the failure of sample. However, with test DT283, because of the higher confining pressure, the shear wave velocity varies slightly even though the soil is sheared to fail. This fact indicates that the highest shear wave speed could be an indicator of shear strength or shear failure state. This phenomenon is not fortuitous and two mechanisms may explain the behavior of velocities during shearing samples.

Shear wave actually is the vibration caused by shear stress and propagates through the soil skeleton. Such a conduction of shear stress depends on the particle contact. If the particle contact is too weak, the shear stress acting on a soil particle can not be transmitted fully to the adjacent ones. In addition, if the number of contacts is

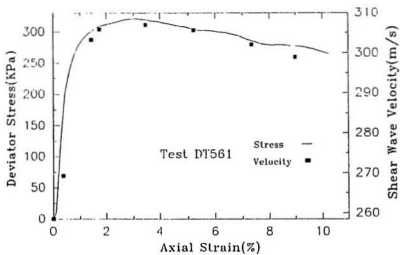
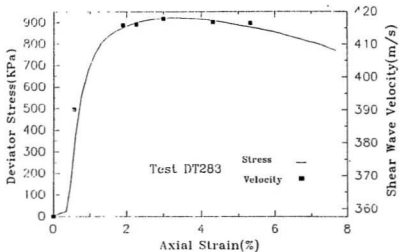


Figure 5.10: Stress-Strain-Velocity Relation(DT561 and DT283)

very small, a soil particle could slip slightly because of the shear stress. Immediate transmittal of vibration to the nearby area is impossible. The results are loss in energy and hence a drop in the propagation speed. In the initial stage of shearing, because an increase of effective stress means that the grains within the mineral skeleton are pressed more tightly together, it becomes increasingly harder to cause sliding between the grains. Also the contact points are increased because of the higher ambient stress. The shear wave velocity therefore increases. Higher confining pressures cause faster shear wave speed.

However, when the soil is sheared close to failure, large strains and rearrangement of the soil structure are required to mobilize the friction. Within this stage, the soil particles can rotate a little around their contact points and thus, they will not contribute to resistance against further movements. Therefore, in the weak area, a shear banding is formed. The formation of shear bands in triaxial specimens is a common occurrence generally assumed to be associated with failure of the specimen. Within the shear band, particle contact becomes very weak and the number of contacts also decreases. The shear banding area rapidly becomes weaker than the remaining major parts of the specimen. Therefore, soil can not resist further axial loading. Similarly the shear stress by vibration can not easily transmit through the shear band because the soil in the shear band seems in a state similar to liquefaction that acts as a buffer and absorbs energy, which causes a drop in shear wave velocity. The formation of shear band depends on the confining pressure. The lower the confining pressure, the quicker the formation of shear band. Therefore, the shear wave velocity in the sample under the lower confining pressure drops faster than the shear wave velocity does in

the sample under the higher confining pressure. Also in figure(5.10), we can also see that the relative density has the similar effects on shear wave velocity development with axial strain.

### 5.3 Correlation of Strength and Wave Velocity

From the above results and descriptions we can see that shear wave velocity-axial strain relationship follows the same mechanism controlling stress-strain behavior of sands. Although shear strength is a large deformation property and shear wave is a small deformation excitation, they are intrinsically correlated. Actually, shear wave is the manifestation of shear stress transmitting. On the other hand, the foregoing experimental results macroscopically indicate that not only does the maximum shear wave velocity coincide with the peak of the stress-strain curve but also the entire velocity-strain curve takes the shape similar to the stress-strain curve. These extraordinary similarities reveal the possibility of using equation(5.2) to correlate strength, strain and shear wave velocity into an integral from which the strength characteristics of a soil could be predicted by measuring acoustic properties, for example, shear wave velocities in this research.

The variations of velocity as a function of triaxial stress are closely dependent on three parameters: the ratio of the principle stresses, the axial strain developed during shearing, and the direction of application of the stress in relation to the propagation direction of the waves analyzed. Synthesizing preceding experimental results and analyses, the following equation is introduced to model shear wave velocity-stress ratio-strain

relationship:

$$\frac{V_s}{(V_s)_0} = 1 + \alpha(1 + d\varepsilon)^{\frac{a}{a+b}} \frac{\varepsilon}{a + b\varepsilon} \left(\frac{\sigma_1}{\sigma_3} - 1\right)^n \quad (5.6)$$

in which  $(V_s)_0$  is the shear wave velocity corresponding to zero axial strain.  $(V_s)_0$  can be obtained from direct measurement or calculated from equation(5.5). All parameters are the same as used in equation(5.2) except that  $\alpha$  is a new parameter introduced.  $\alpha$  can be obtained from regression analyses. It varies between 0.026 and 0.090.

As a comparison, the measured data in figure(5.10) are plotted again in figure(5.11). Numerical data are also presented in the figure. It can be seen that the proposed model can fit very well the measured data. Because  $(V_s)_{max}$  corresponds to the axial strain at failure and the peak strength of the sample, if  $(V_s)_{max}$  and  $\varepsilon_f$  are substituted into equation(5.6), the maximum stress ratio can be calculated from acoustic measurements. Other experimental results are included in the Appendix B. Some discrepancies exist in the tests under low confining pressures. However, when the confining pressure is higher, the measured data are close to the model curve. Those figures and tables indicate good agreement between the measured strength and the calculated strength from model.

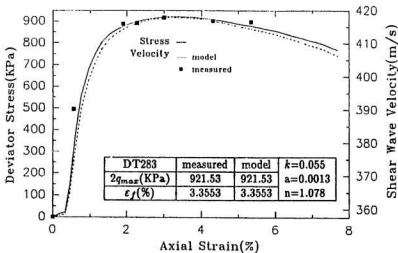
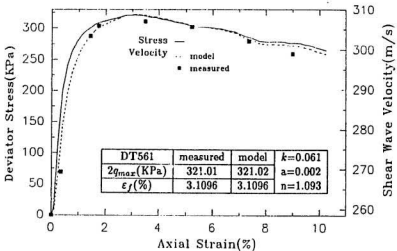


Figure 5.11: Comparison of Model and Test Data(DT561 and DT283)

## Chapter 6

# Summary and Conclusions

No honest business man and no self-respecting scientist can be expected to put forth a new scheme or a new theory as a "working proposition" unless it is sustained by at least fairly adequate evidence.

K. Terzaghi[113]

In order to overcome the shortcomings in the conventional correlation techniques, a combined laboratory acoustic-triaxial machine was modified to measure shear strength and shear wave velocity at the same time. The piezoelectric ceramic benders were used as shear wave transmitter and receiver. The wave propagation time was determined by both oscilloscope and Hilbert transform. *Forty tests were conducted under various conditions of soil type, relative density, confining pressure and acoustic signal frequency.*

Based on the strength experimental results, an unified stress-strain model was proposed to predict soil behavior under loading condition. It can be seen that the popular hyperbolic model is a special case of the new model. The proposed equation requires five parameters. However, it is found in this study that three of these parameters do not change with different conditions. The other two parameters depend on the con-

*fining pressure, soil type, relative density.* The stress strain curves predicted from the model show *good agreement* with those obtained from the experimental data.

Before the sample is sheared, the measured shear wave velocity is found varying with void ratio and confining pressure. An empirical equation was developed. This equation predicts linear decrease in wave velocity with void ratio and nonlinear increase with confining pressure. Velocities vary rather slightly with acoustic signal frequency.

Although the shear strength is a large deformation property of a soil and acoustic measurement is from a small deformation excitation, they are connected in the sense of microbehavior. The same mechanism controls both of them. It is observed in this study that the stress strain curve is quite similar to that of shear wave velocity versus strain. In the first stage of shearing, the shear wave velocity increases with increasing axial strain. The shear wave velocity reaches its peak value almost at the same moment as the deviator stress does. The current test results provide a wealth of information on the correlations between strength and shear wave velocity. Therefore, the proposed constitutive equation was further modified and introduced to reconcile experiment results and theory. Comparisons between the estimated strength values and those obtained in the tests render compelling evidence that shear strength can be obtained from the proposed models.

However, the results from this laboratory research can not yet be directly employed to the in-situ application. Especially, it remains to understand the factors influencing parameters required by the new models. Further research must be pursued both

in the laboratory and in-situ. The effect of changing shear rate was not studied in this program. In addition, a wide range of soil types, relative densities and confining pressures should be used to validate and improve the proposed model. The combined acoustic-triaxial-resonant column test is recommended for future study.

## Bibliography

- [1] K.Terzaghi, and R.B.Peck, *Soil Mechanics in Engineering Practice*. John Wiley, New York, 1968, 729p.
- [2] R.E.Sherief, *Geophysical Methods*. Prentice Hall, New Jersey, 1989, 605p.
- [3] R.D.Woods, and K.H.Stokoe,II, "Shallow Seismic Exploration in Soil Dynamics", in *Richard Commemorative Lectures*, ed. R.D.Woods, ASCE, 1985, pp.120-156.
- [4] T.G.Muir, "Nonlinear Acoustics and Its Role in the Sedimentary Geophysics of the Sea", in *Physics of Sound in Marine Sediments*, ed. L.Hampton, Plenum Press, New York, 1974. pp.241-291.
- [5] S.Lacasse, and T.Berre. "Triaxial Testing Methods for Soils". in *Advanced Triaxial Testing of Soil and Rock*, eds. R.T.Douaghe. R.C.Chaney. and M.L.Silver, ASTM, STP977, 1988. pp.264-289.
- [6] C.R.Bates, "Dynamic Soil Properties Measurements during Triaxial Testing". *Geotechnique*, Vol.39, No.4, 1989. pp.721-726.
- [7] C.P.Wroth, and D.M.Wood, "The Correlation of Index Properties with Some Basic Engineering Properties of Soils". *Can. Geotech. J.*, Vol.15. 1978, pp.137-145.
- [8] J.Y.Guigne, G.B.Crocker, and P.Hunt, "Non-linear Acoustic Imaging of Ice Properties". *J. of Glaciology*. Vol.38, No.128, 1991, pp.93-100.
- [9] N.A.Cochrane, "Automatic Marine Sediment Acoustic Classification", in *Automatic Marine Sediment Classification*, ed. N.A.Cocheane, Ocean Engineering Center, Memorial Univ. of Newfoundland, 1980, Vol.2.
- [10] S.T.Abdel-gawad, Correlation Between Geotechnical and Acoustic Properties of Marine Sediments-Outer Placentia Bay, Newfoundland. *Master Thesis*, Faculty of Engrg. and Applied Sci., Memorial Univ. of Nfld., 1980.
- [11] J.I.Clark, and J.Y.Guigne, "Marine Geotechnical Engineering in Canada", *Can. Geotech. J.*, Vol.25, 1988. pp.179-198.
- [12] J.Y.Guigne, and V.H.Chin, "Acoustic Imaging of an Inhomogeneous Sediment Matrix", *Marine Geophysical Researches*, Vol.11, 1989, pp.301-317.

- [13] J.Y.Guigne, V.H.Chin, and S.M.Solomon, "Acoustic Attenuation Measurements Using Parametric Arrays", *Ultrasonics*, Vol.27, 1989, pp.297-301.
- [14] J.Y.Guigne, The Concept, Design and Experimental Evaluation of an "Acoustic Sub-seabed Interrogator". *Ph.D. Thesis*, University of Bath, 1986.
- [15] J.Y.Guigne, C.J.Pike, and S.T.Inkpen, "IMAP-Interactive Marine Acoustic Probe: Acoustic Site Evaluation, Terrenceville, Newfoundland". *C-CORE Technical Report*, C-CORE Publication No.91-31, September, 1991.
- [16] J.H.Schmertmann, "Measurement of In-situ Shear Strength", in *Procs. of the Conf. on In-situ Measurement of Soil Properties*, Vol.2, ASCE, 1976, pp.57-179.
- [17] U.S. Department of Commerce, Present and Recommended U.S. Government Research in Seafloor Engineering, Washington, 1978, 93p.
- [18] H.J.Lee, "The role of Laboratory Testing in the Determination of Deep-sea Sediment Engineering Properties", in *Deep-sea Sediments: Physical and Mechanical Properties*, ed. A.L.Underbitzen, Plenum Press, New York, 1974, pp.111-127.
- [19] L.Bjerrum, "Problems of Soil Mechanics and Construction on Soft Clays and Structurally Unstable Soils(Collapsible, Expansive and Others)", *Proc. of 8th ICSMFE*, Vol.3, 1973, Session 4, pp.111-153.
- [20] D.R.Burns, "Acoustic Waveform Logs and the In-situ Measurement of Permeability—a Review", in *Geophysical Applications for Geotechnical Investigations*, eds. F.L.Paillet, and W.R. Saunders, ASTM, STP 1101, 1990, pp.65-78.
- [21] D.T.Smith, "Geotechnical Characteristics of the Sea Bed Related to Seismo-acoustics", in *Ocean Seismo-acoustics: Low Frequency Underwater Acoustics*, eds. T.Akal, and J.M.Berkson, Plenum Press, New York, 1986, pp.483-500.
- [22] M.A.Biot, "Theory of Propagation of Elastic Waves in a Fluid-saturated Porous Solid", *J. Acoust. Soc. Am.*, Vol.28, 1956, pp.168-191.
- [23] D.C.Ontwisle, and D.M.McCann, "An Assessment of the Use of Christensen's Equation for the Prediction of Shear Wave Velocity and Engineering Parameters", in *Geological Applications of Wireline Logs*, eds. A.Hurst, M.A.Lovell, and A.C.Morton, Geological Society Special Publication No.48, London, 1990, pp.347-354.
- [24] R.J.Hoar, and K.H.Stokoe II, "Generation and Measurement of Shear Waves In-situ", in *Dynamic Geotechnical Testing*, ASTM, STP654, 1978, pp.3-29.
- [25] K.Tokimatsu, and S.Tamura, "V<sub>s</sub> Determination from Steady State Rayleigh Wave Method", *Soil and Foundations*, Vol.31, No.2, 1991, pp.153-163.
- [26] S.Ohya, S.Imai, and M.Nagura, "Recent Developments in Pressuremeter Testing, In-situ Stress Measurement and S-wave Velocity Measurement", in *Recent Developments in Laboratory and Field Tests and Analysis of Geotechnical Problems*, eds. A.S.Balasubramaniam, S.Chandra, and D.T.Bergado, A.A.Balkema, Rotterdam, 1986, pp.189-209.

- [27] G.N.Smith, Elements of Soil Mechanics. BSP Professional Books, Boston, 6th edition, 1990, 509p.
- [28] D.J.Murphy, "Stress, Degradation, and Shear Strength of Granular Material", in *Geotechnical Modeling and Applications*, ed. S.M.Sayed, Gulf Publishing Co., 1987.
- [29] M.C.Ervin, In-situ Testing for Geotechnical Investigations. A.A.Balkema, Rotterdam, 1983, 131p.
- [30] R.J.Mair, and D.M.Wood, Pressuremeter Testing: Methods and Interpretation. Butterworths, 1987, 160p.
- [31] G.W.Clough, J.L.Briaud, and J.M.O.Hughes, "The Development of Pressuremeter Testing", in *Pressuremeters*, Proc. of the 3rd Int. Symposium on Pressuremeters, Thomas Telford Ltd., London, 1990, pp.25-46.
- [32] A.F.Richards, Vane Shear Strength Testing in Soils: Field and Laboratory Studies. ASTM, STP1014, 1988, 376p.
- [33] J.Dunnichiff, Geotechnical Instrumentation for Monitoring Field Performance. John Wiley & Sons, New York, 1988, 577p.
- [34] K.Tanimoto, and J.Nakamura, "Studies of Acoustic Emission in Soil", in *Acoustic Emissions in Geotechnical Engineering Practice*, eds. V.P.Drnevich, and R.E.Gray, ASTM, STP 750, 1981, pp.161-173.
- [35] R.V.Williams, Acoustic Emission, Adam Hilger Ltd., Bristol, 1980, 118p.
- [36] R.C.Chaney, K.R.Demars, and H.Y.Fang, "Toward a Unified Approach to Soil Property Characterization: In Situ Versus Laboratory", in *Strength Testing of Marine Sediments: Laboratory and In-situ Measurements*, eds. R.C.Chaney, and K.R.Demars, ASTM, STP883, 1986, pp.425-439.
- [37] G.Baldi, D.W.Hight, and G.E.Thomas, "A Reevaluation of Conventional Triaxial Test Methods", in *Advanced Triaxial Testing of Soil and Rock*, eds. R.T.Donaghe, R.C.Chaney, and M.L.Silver, ASTM, STP 977, 1988, 896p.
- [38] R.N.Yong, and M.M.Tabba, "On the Random Aspect of Shear Strength", in *Laboratory Shear Strength of Soil*, eds. R.N.Yong and F.C.Townsend, ASTM, STP 740, 1981, 717p.
- [39] T.Ueng, Y.Tzon, and C. Lee, "The Effect of End Restraint on Volume Change and Particle Breakage of Sands in Triaxial Tests", in *Advanced Triaxial Testing of Soil and Rock*, eds. R.T.Donaghe, R.C.Chaney, and M.L.Silver, ASTM, STP 977, 1988, pp679-691.
- [40] Y.P.Vaid, and D.Negussey, "A Critical Assessment of Membrane Penetration in the Triaxial Test", *Geotech. Testing J.*, Vol.7, No.2, 1984, pp.70-76.

- [41] R.H.Kuerbis, and Y.P.Vaid. "Corrections for Membrane Strength in the Triaxial Test", *Geotech. Testing J.*, Vol.13, No.4, 1990, pp.361-369.
- [42] F.Tatsuoka, "Some Recent Developments in Triaxial Testing Systems for Cohesionless Soils", in *Advanced Triaxial Testing of Soil and Rock*, eds. R.T.Donaghe, R.C.Chaney, and M.L.Silver, ASTM, STP 977, 1988, pp.7-67.
- [43] S.Roesler, "Correlation Methods in Soil Dynamics", in *Dynamical Methods in Soil and Rock Mechanics*, ed. B. Prange, Proc. of DMSR 77, Vol.1, A.A.Balkema, Rotterdam, 1978, pp.309-334.
- [44] B.O.Hardin, and F.E.Richert, Jr., "Elastic Wave Velocities in Granular Soils", *J. Soil Mech. and Found. Div.*, ASCE, Vol.89, No.SM1, 1963, pp.33-65.
- [45] K.Saiki, "An Attempt to Relate Physical Index Properties with Undrained Shear Strength of Saturated Tigris Basin Clays", in *Recent Developments in Laboratory and Field Tests and Analysis of Geotechnical Problems*, eds. A.S.Balasubramaniam, S.Chandra, and D.T.Bergado, A.A.Balkema, Rotterdam, 1986, pp.333-335.
- [46] A.S.Laughto, "Sound Propagation in Compacted Ocean Sediments", *Geophysics*, Vol.22, No.2, 1957, pp.233-260.
- [47] F.V.Lawrence, Jr., "Propagation Velocity of Ultrasonic Waves through Sand. MIT Research Report R63-8, 1963.
- [48] R.W.Stephenson, "Ultrasonic Testing for Determining Dynamic Soil Moduli", in *Dynamic Geotechnical Testing*, ASTM, STP654, 1978, pp.179-195.
- [49] R.D.Stoll, "Effects of Gas Hydrates in Sediments", in *Natural Gases in Marine Sediments*, ed. I.R.Kaplan, Plenum Press, New York, 1974, pp.235-248.
- [50] C.C.Leroy, J.M.Dauplex, and P.J.Longuemard, "Relationship Between the Acoustical Characteristics of Deep Sea Sediments and Their Physical Environment", in *Ocean Seismo-acoustics: Low Frequency Underwater Acoustics*, eds. T.Akal, and J.M.Berkson, Plenum Press, New York, 1986, pp.511-517.
- [51] T.B.Edil, and G.F.Luh, "Dynamic Modulus and Damping Relationships for Sands", in *Earthquake Engineering and Soil Dynamics*, Proc. of the ASCE Geotechnical Engineering Division, 1978, Vol.1, pp.391-409.
- [52] H.Seed, and I.M.Idriss, *Soil Moduli and Damping Factors for Dynamic Response Analyses. Report EERC70-10, Earthquake Engineering Research Center, Univ. of California at Berkeley, 1970.*
- [53] K.H.Stokoe II, S.H.H.Lee, and D.P.Knox, "Shear Moduli Measurements under True Triaxial Stresses", in *Advances in the Art of Testing Soils under Cyclic Conditions*, ed. V.Khosla, ASCE, 1985, pp.166-185.
- [54] S.K.Roesler, "Anisotropic Shear Modulus due to Stress Anisotropy", *J. of Geotechnical Engrg.*, Vol.105, No.GT7, 1979, pp.871-881.

- [55] P.Yu, and F.E.Richart, "Stress Ratio Effects on Shear Modulus of Dry Sands", *J. of Geotechnical Engrg.*, Vol.110, No.3, 1984, pp.331-345.
- [56] P.J.Schultheiss, "The Influence of Packing Structure and Effective Stress on  $V_p$ ,  $V_s$ , and the Calculated Dynamic and Static Moduli in Sediments", in *Acoustics and the Sea-bed*, ed. N.G.Pace, Bath University Press, 1983, pp.19-27.
- [57] P.J.Schultheiss, "Simultaneous Measurement of P & S Wave Velocities During Conventional Laboratory Soil Testing Procedures", *Marine Geotechnology*, Vol.4, No.4, 1981, pp.343-367.
- [58] S.Nishio, and K.Tamaoki, "Stress Dependency of Shear Wave Velocities in Diluvial Gravel Samples During Triaxial Compression Tests", *Soil and Foundations*, Vol.30, No.4, 1990, pp.42-52.
- [59] T.Imai, and K.Yokota, "Relationships between N value and Dynamic Soil Properties", *Proc. of 2nd European Symposium on Penetration Testing*, Amsterdam, 1982, pp.73-78.
- [60] J.H.Schmertmann, "Use the SPT to Measure Dynamic Soil Properties?—Yes. But...!", in *Dynamic Geotechnical Testing*, ed. M.L.Silver, ASTM, 1978. STP 654, pp.341-355.
- [61] K.Tokimatsu, and A.Uchida, "Correlation between Liquefaction Resistance and Shear Wave Velocity", *Soils and Foundations*, Vol.30, No.2, 1990, pp.33-42.
- [62] P.D.Alba, K.Baldwin, V.Janoo, G.Roe, and B.Celikkol, "Elastic-Wave Velocities and Liquefaction Potential", *Geotech. Testing J.*, Vol.7, No.2, 1984, pp.77-87.
- [63] K.C.Baldwin, and P.D.Alba, "Use of Shear and Compressional Waves to Determine Liquefaction Resistance of Sand", in *The Correlation of Acoustic and Physical Properties of Marine Sediments*, ed. P.G.Simpkin, Proc. of the Acoustic-geotechnical Correlation Workshop, 1984, pp.23-34.
- [64] S.H.Bolton, "Evaluation of the Dynamic Characteristics of Sands by In-situ Testing Techniques", in *Revue Francaise de Geotechnique*, No.23, 1983. Paris, Vol.3, pp.91-99.
- [65] M.F.Kaplan, "The Relation Between the Ultrasonic Pulse Velocity and the Compressive Strength of Concretes Having the same Workability but Different Mix Properties", *Mag. of Concrete Res.*, 1960, Vol.12, No.34.
- [66] W.D.Carrier III, and J.F.Brechman, "Correlations between Index Tests and the Properties of Remoulded Clays", *Geotechnique*, Vol.34, No.2, 1984, pp.211-228.
- [67] G.V.Keller, "Resistivity Surveys and Engineering Problems", in *Geophysical Methods in Geotechnical Engineering*, ASCE National Convention, 1979, pp.1-50.
- [68] R.A.Sullivan, and S.J.Wright, and D.W.F.Semner, "Evaluation of Design Parameters from Laboratory Tests", in *Offshore Site Investigation*, ed. D.A.Ardus, Graham & Trotman, 1979, pp.201-215.

- [69] L.S.Lee, and G.B.Baecher, Acoustic Data and Uncertainty in Geotechnical Site Characterization Offshore. MIT Report No. MITSG 83-13, 1983, 188p.
- [70] G.H.Sutton, H.Bereckhemer, and J.E.Nafe, "Physical Analysis of Deep Sea Sediments", *Geophysics*, Vol.22, No.4, 1957, pp.779-812.
- [71] L.D.Bely, G.N.Nazarov, E.V.Chebkasova, and A.N.Chu-machenko, "Seismic Methods for Study of Soil Building Properties", *Bulletin of the Int. Assoc. of Engrg. Geology*, No.26-27, Paris, Vol.1, 1983, pp.107-109.
- [72] R.D'Andrea, In-situ Shear Strength Characteristics of a Stratified Silt, M.S. Thesis, Dept. Civil. Engr., Univ. of Rhode Island, 1966, 62p.
- [73] S.Buchan, F.C.D.Dewes, D.M.McCam, and D.T.Smith, "Measurements of the Acoustic and Geotechnical Properties of Marine Sediment Cores", in *Marine Geotechnique*, ed. A.F.Richards, Univ. of Illinois Press, 1967, pp.65-92.
- [74] B.DeRoock, and A.W.Cooper, "Relation Between Propagation Velocity of Mechanical Waves Through Soil and Soil Strength", *Proc. of Int. Symposium on Wave Propagation and Dynamic Properties of Earth Materials*, ed. G.E.Triandafilidis, Univ. of New Mexico Press, 1967, pp.905-912.
- [75] D.R.Horn, B.M.Horn, and M.N.Delach, "Correlation Between Acoustical and Other Physical Properties of Deep-sea Cores", *J. of Geophysical Research*, Vol.73, No.6, 1968, pp.1939-1957.
- [76] B.Denness, D.M.McCam, and A.Fairlie, "Geotechnical Studies of the Sea Floor Sediments around Arran", in *Offshore Structures*, ed. J.P.Blanc, 1974, pp.21-26.
- [77] A.Hara, T.Ohta, M.Niwa, S.Tanaka, and T.Banno, "Shear Modulus and Shear Strength of Cohesive Soils", *Soils and Foundations*, Vol.14, No.3, 1974, pp.1-12.
- [78] V.A.Nacci, M.C.Wang, and J.Gallagher, "Influence of Anisotropy and soil Structure on Elastic Properties of Sediments", in *Physics of Sound in Marine Sediments*, ed. L.Hampton, Plenum Press, New York, 1974, pp.63-87.
- [79] Y.S.Chae, and J.C.Chiang, "Dynamic Properties of Lime and LFA Treated Soils", in *Earthquake Engineering and Soil Dynamics*, Proc. of the ASCE Geotechnical Engineering Division, 1978, Vol.1, pp.308-324.
- [80] S.K.Saxena, A.S.Avramidis, and K.R.Reddy, "Dynamic Moduli and Damping Ratios of Cemented Sands at Low Strains", *Can. Geotech. J.* Vol.25, 1988, pp.353-368.
- [81] B.Zhang, and C.Lin, "Shear Wave Velocity and Geotechnical Properties of Tailings Deposits", *Bulletin of Int. Assoc. of Engrg. Geology*, No.26-27, Vol.1, 1983, pp.347-353.
- [82] K.Tononchi, T.Sakayama, and T.Imai, "S Wave Velocity in the Ground and the Damping Factor", *Bulletin of the Int. Assoc. of Engrg. Geology*, No.26-27, Paris, Vol.1, 1983, pp.327-333.

- [83] M.B.Dussault, "The Use of Geophysical Logs in Geotechnical Engineering", *Proc. of 39th Canadian Geotechnical Conf.*, 1986, pp.29-40.
- [84] R.J.Lorimer, T.M.McGee, and R.A.Spence, "A Comparison of Acoustically and Mechanically Determined Shear Characteristics of a Marine Soil", *Proc. of 3rd Canadian Conf. on Marine Geotechnical Engrg.*, St. John's, Vol.2, 1986, pp.541-555.
- [85] E.L.Hamilton, "Prediction of Deep-sea Sediment Properties: State-of-the Art", in *Deep-sea Sediments: Physical and Mechanical Properties*, ed. A.L.Inderbitzen, Plenum Press, New York, 1974, pp.1-44.
- [86] E.L.Hamilton, "Sound Velocity and Related Properties of Marine Sediments, North Pacific", *J. of Geophysical Research*, Vol.75, No.23, 1970, pp.4423-4446.
- [87] E.L.Hamilton, and R.T.Bachman, "Sound Velocity and Related Properties of Marine Sediments", *J. Acoust. Soc. Am.*, Vol.72, No.6, 1982, pp.1891-1904.
- [88] D.T.Smith, "Acoustic and Mechanical Loading of Marine Sediments", in *Physics of Sound in Marine Sediments*, ed. L.Hampton, Plenum Press, New York, 1974, pp.41-61.
- [89] B.S.Fedders, and G.H.Ziehm, "Determination of the Acoustic Properties of the Sea-floor by Measuring the Electric Impedance of a Transducer", in *Acoustics and Seabed*, ed. N.G.Pace. Univ. of Bath Press, 1983, pp.91-96.
- [90] D.J.Shirley, "Method for Measuring in-situ Acoustic Impedance of Marine Sediments", *J. Acoust. Soc. Am.*, Vol.62, No.4, 1977, pp.1028-1032.
- [91] E.Bamert, G.Schmitter, and M.Weber, "Triaxial and Seismic Laboratory Tests for Stress-strain-time Studies". *Proc. of Conf. of 6th ICSMFE*, 1965, Vol.1, pp.151-155.
- [92] J.E.Nafe, and C.L.Drake, "Physical Properties of Marine Sediments", in *The Sea: Ideas and Observations on Progress in the Study of the Seas*, Vol.3, Interscience Publishers, 1963, pp.794-815.
- [93] R.V.Whitman, E.T.Miller, and P.J.Moore, "Yielding and Locking of Confined Sand", *J. Soil and Foundation Div.*, ASCE, Vol.90, SM4, 1964, pp.57-84.
- [94] M.D.Bolton, and J.M.R.Wilson, "An Experimental and Theoretical Comparison between Static and Dynamic Torsional Soil Tests". *Geotechnique*, Vol.39, No.4, 1989, pp.585-599.
- [95] C.P.Wroth, "The Interpretation of In-situ Soil Tests", *Geotechnique*, Vol.34, No.4, 1984, pp.449-489.
- [96] D.W.Hight, A.Gens, T.M.P.De Campos, and M.Takahashi, "Factors Influencing the Interpretation of In-situ Strength Tests in Insensitive Low Plasticity Clays", *Proc. of the 3rd Int. Conf. on Behavior of Off-shore Structures*, Vol.2, eds. C.Chrysostomidis, and J.J.Connor, 1982, pp.438-450.

- [97] C.C.Ladd, Discussion on "In-situ Measurement of Shear Strength" by J. Schmertmann, *Procs. of the Conf. on In-situ Measurement of Soil Properties*, Vol.2, ASCE, 1976, pp.153-160.
- [98] C.P.Wroth, "Correlations of Some Engineering Properties of Soils", *Procs. of 2nd Int. Conf. on Behavior of Off-shore Structures*, 1979, pp.121-132.
- [99] N.Janbu, Discussion on "In-situ Measurement of Shear Strength" by J. Schmertmann, *Procs. of the Conf. on In-situ Measurement of Soil Properties*, Vol.2, ASCE, 1976, pp.150-152.
- [100] T.G.Thomann, and R.D.Hryciw, "Laboratory Measurement of Small Strain Shear Modulus under  $K_0$  Conditions", *Geotech. Testing J.*, Vol.13, No.2, 1990, pp.97-105.
- [101] C.R.Bates, "Dynamic Soil Properties Measurements during Triaxial Testing", *Geotechnique*, Vol.39, No.4, 1989, pp.721-726.
- [102] R.Dyvik, and C.Madhus, "Lab Measurements of  $G_{max}$  using Bender Elements", in *Advances in the Art of Testing Soils under Cyclic Conditions*, ed. V.Khosla, ASCE, 1985, pp.186-196.
- [103] A.W.Bishop, and D.J.Henkel, *The Measurement of Soil Properties in The Triaxial Test*, Edward Arnold Ltd., London, 1964, 228p.
- [104] A.B.Wood, *A Textbook of Sound*, G.Bell & Sons, London, 1964, 610p.
- [105] T.F.Huetter, and R.H.Bolt, *Sonics: Techniques for the Use of Sound and Ultrasound in Engineering and Science*, John Wiley & Sons, 1966, 455p.
- [106] D.J.Shirley, and L.D.Hampton, "Shear-wave Measurements in Laboratory Sediments", *J. Acoust. Soc. Am.*, Vol.63, No.2, Feb., 1978, pp.607-613.
- [107] D.J.Shirley, "An Improved Shear Wave Transducer", *J. Acoust. Soc. Am.*, Vol.63, No.5, May, 1978, pp.1643-1645.
- [108] R.Dyvik, and C.Madhus, "Lab Measurements of  $G_{max}$  Using Bender Elements", in *Advances in the Art of Testing Soils Under Cyclic Conditions*, ed. V.Khosla, ASCE, 1985, pp.186-196.
- [109] Y.P.Vaid, and D.Negussey, "Preparation of Reconstituted Sand Specimens", in *Advanced Triaxial Testing of Soil and Rock*, ed. R.T.Donaghe, R.C.Chaney, and M.L.Silver, ASTM, 1988, STP 977, 896p.
- [110] M.T.Taner, F.Koehler, and R.E.Sheriff, "Complex Seismic Trace Analysis", *Geophysics*, Vol.44, No.6, 1979, pp.1041-1063.
- [111] R.N.Bracewell: *The Fourier Transform and Its Application*, McGraw-Hill Book Co., 1978, 2nd edition, 444p.
- [112] P.A.Baran, and P.M.Sweezy, *Monopoly Capital: an Essay on the American Economic and Social Order*, Monthly Review Press, New York, 1969, 402p.

- [113] K. Terzaghi, Presidential Address given at 1st Int. Conf. on SMFE, 1936, in *From theory to Practice in Soil Mechanics: selections from the writings of Karl Terzaghi*, ed. L. Bjerrum, A. Casagrande, R.B. Peck, and A.W. Skempton, John Wiley & Sons, New York, 1967, pp.62-67.

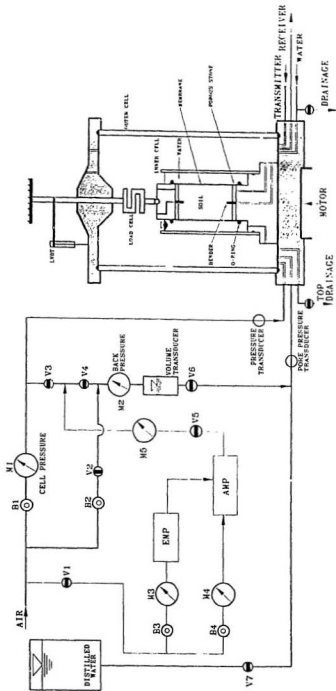
## Appendix A

# Test Procedures and Calibration of Transducers

## A.1 Test Procedures

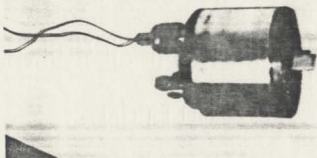
The complete acoustic triaxial device assembly is shown in the figure on the following page. It is important for the user to be familiar with all connections and working principles. Detailed test procedures are described as follows.

# ACOUSTIC TRIAXIAL DEVICE

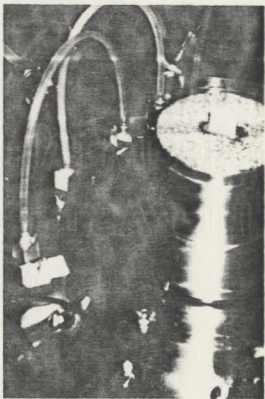


REPRODUCED FROM THE ORIGINAL

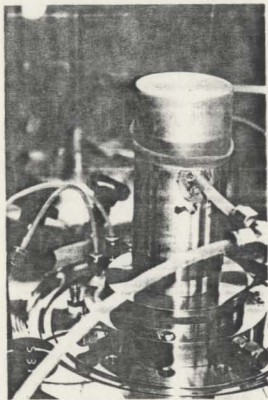
1. Check the cap to make sure the bender element in good condition as shown in the following picture.



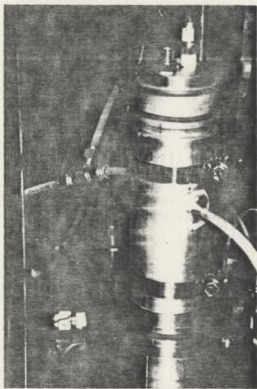
2. Check the pedestal to make sure the bender element in good condition as shown in the following picture.



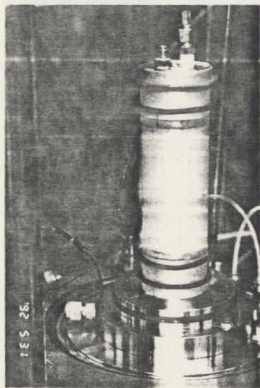
3. Mount sample mold and membrane. Apply vacuum between the membrane and the mold. Fill the mold with premeasured sand. Use air pluviation method to achieve required relative density. Tapping the side of the mold and hand-compaction with a small rod may be used. Make sure the sample is as uniform as possible and the bender element not damaged.



4. Mount cap carefully not to damage the bender element. Remove the vacuum between membrane and the mold.



5. Apply certain vacuum within the sample and then remove the mold.



6. Place the inner cylinder and connect all tubes and electrical wires.



7. Place the outer cylinder. Put on a metal grid guard around the outer cylinder.



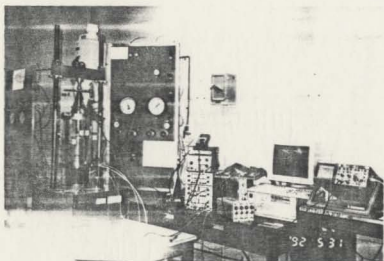
8. Mount the triaxial cell top and the load cell. Fill water into the inner cylinder. If the sample is dry soil, it is not necessary to fill water. Connect triaxial cell with control panel. Apply certain confining pressure in the cell. Remove the vacuum in the sample.



9. Connect all transducers to the proper electrical equipment and data acquisition board in the computer.



10. Check the whole system to make sure everything in good condition. Apply confining pressure to the required value.

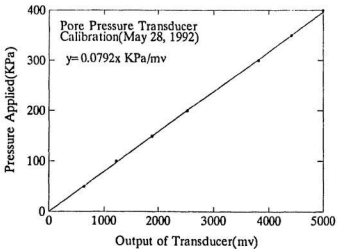
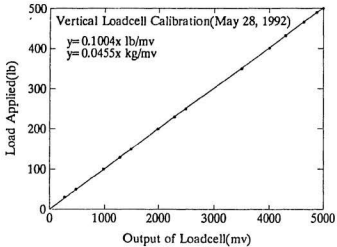


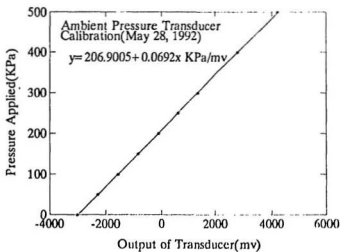
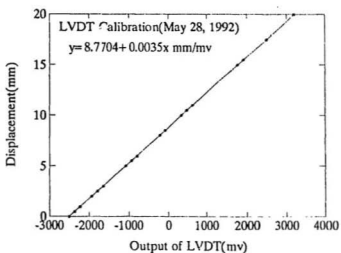
11. Set the axial strain rate to the required value. Check the computer program to make sure each channel works. Start the motor to shear the sample. Start the computer to acquire data.

Input Channel	Tr	Current Value	Scaler Units	Low Limit	High Limit	Range Status	File Setup Done!
CALC 0	LI01	7.85	mm	-1.00	100.00	OK	
CALC 1	FF02	-9.22	ETA	-1.00	400.00	OK	
CALC 2	SL00	250.00	kg	-1.00	250.00	OK	
CALC 3	TS10	6.07	mm	-1.00	100.00	OK	
CALC 4	CP02	290.62	ETA	-1.00	500.00	OK	
CALC 5	UL	0.00	mm <sup>2</sup>	-1.00	100.00		
CALC 6	6	0.00	None	0.00	100.00		
CALC 7	7	0.00	None	0.00	100.00		
CALC 8	8	0.00	None	0.00	100.00		
CALC 9	9	0.00	None	0.00	100.00		
CALC 10	10	0.00	None	0.00	100.00		
CALC 11	11	0.00	None	0.00	100.00		
CALC 12	12	0.00	None	0.00	100.00		
CALC 13	13	0.00	None	0.00	100.00		
CALC 14	14	0.00	None	0.00	100.00		
CALC 15	15	0.00	None	0.00	100.00		

New 2158    Rich-11294    21-00 39  
XXXXXXXXXX    XXXXXXXXXX

## A.2 Transducer Calibration



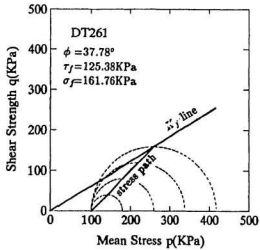
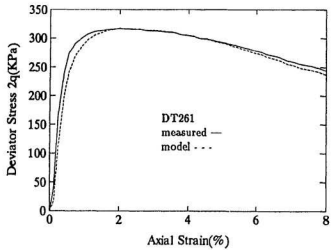


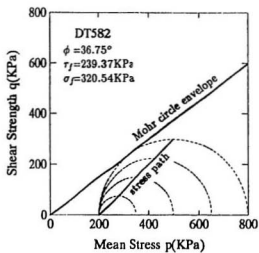
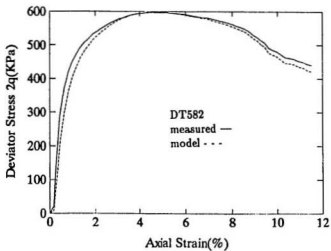
## **Appendix B**

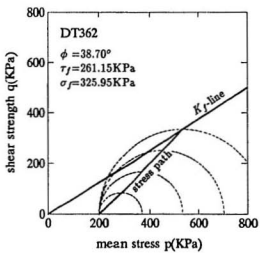
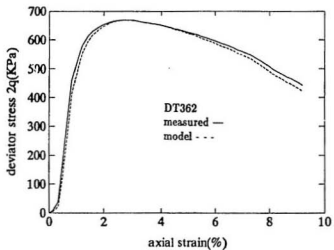
### **Experimental Results**

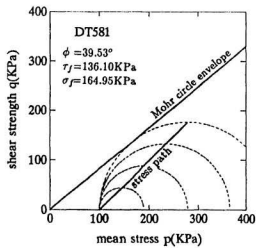
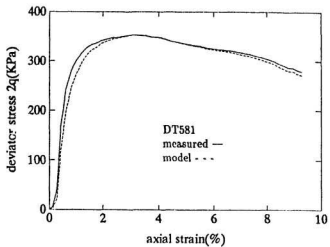
## B.1 Strength Tests

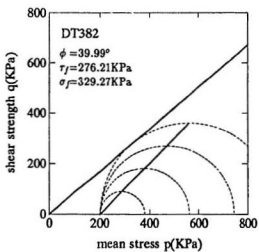
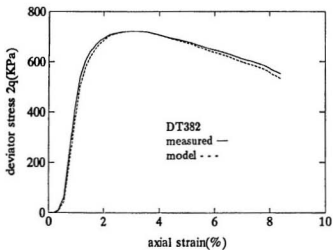
There are two ways to find the value of internal friction angle: (1) construct Mohr circles and draw the Mohr envelope; or (2) plot values of  $p_f$  and  $q_f$ , draw the  $K_f$ -line, and then compute the angle. Both methods are used in the following manipulations of triaxial test data. For the convenience of later comparison, each test in a series is plotted separately. The true internal friction angle should take the average value in the same series.

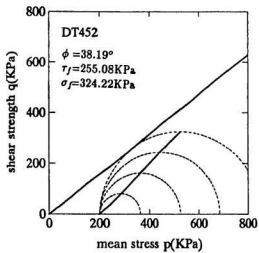
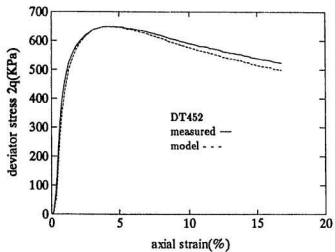


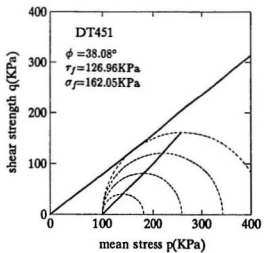
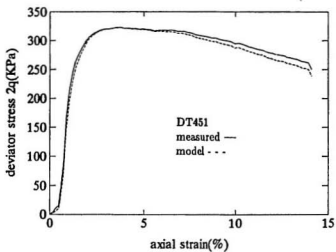


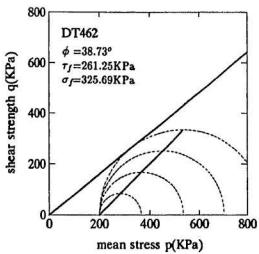
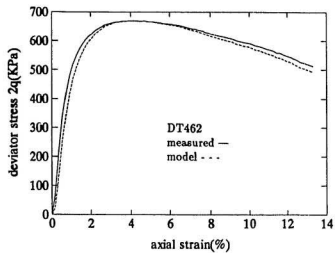


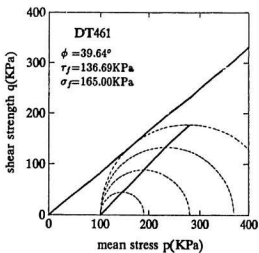
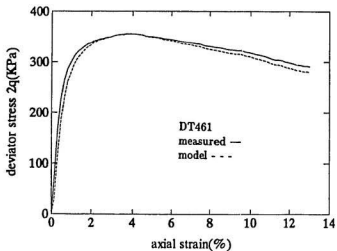


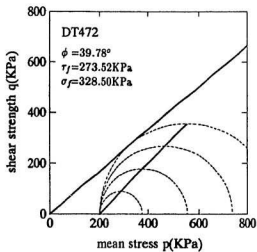
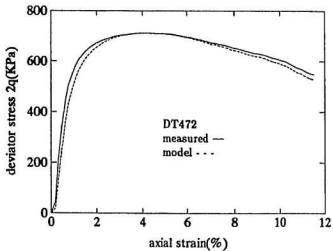


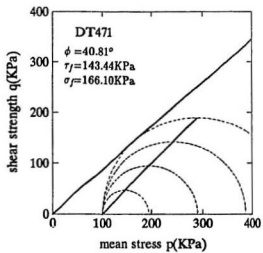
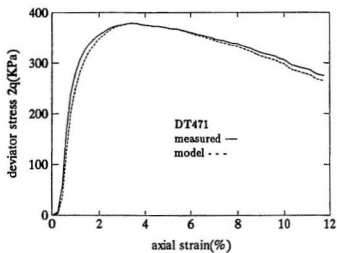


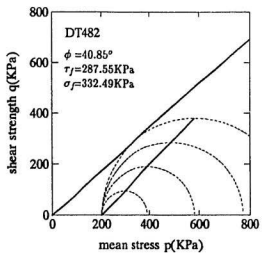
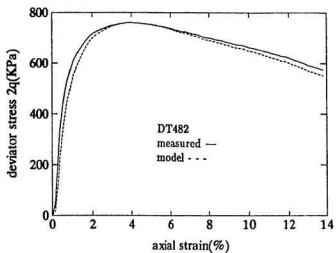


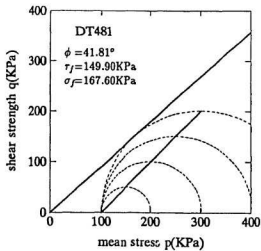
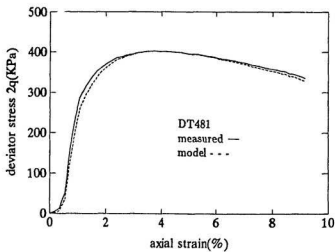


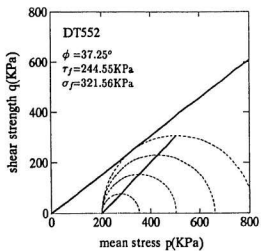
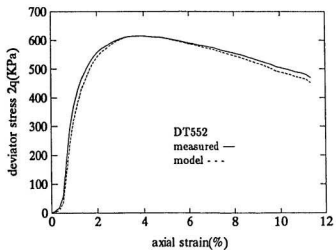


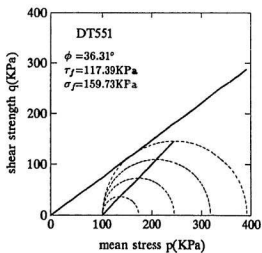
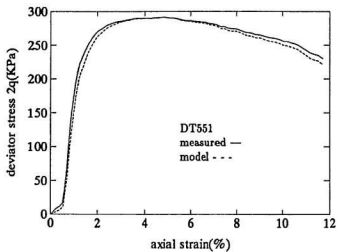


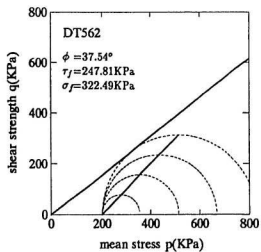
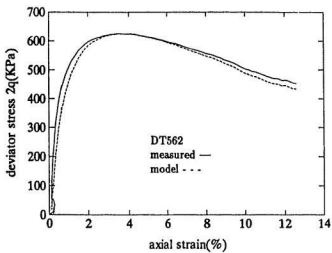


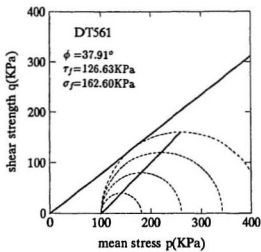
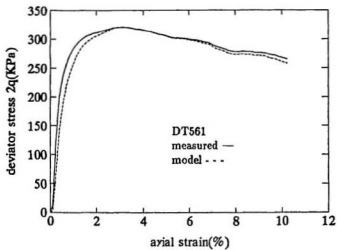


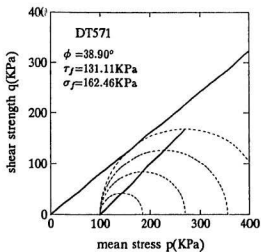
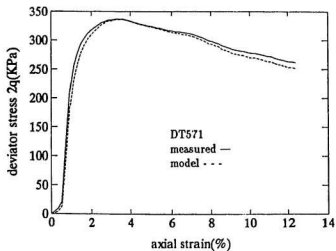


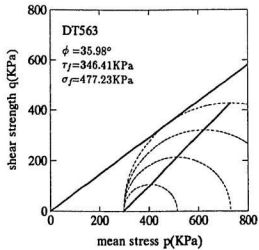
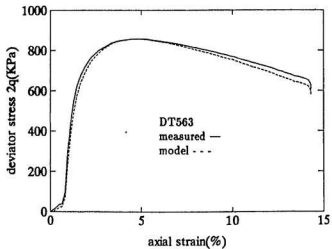


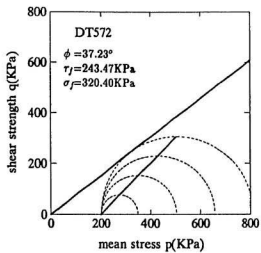
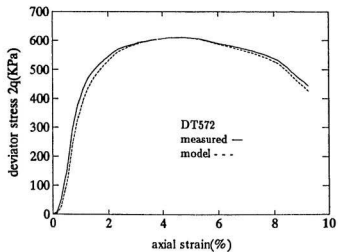


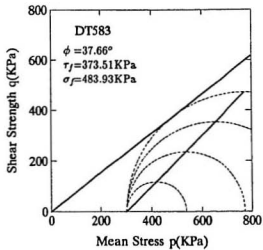
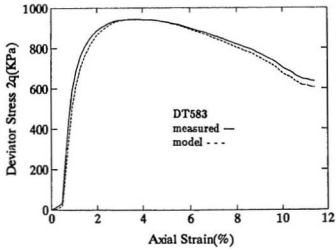


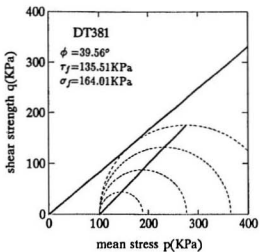
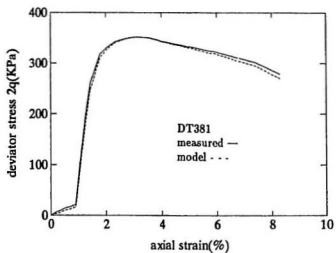


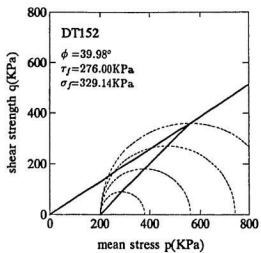
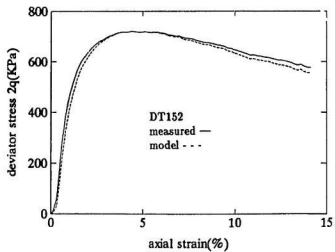


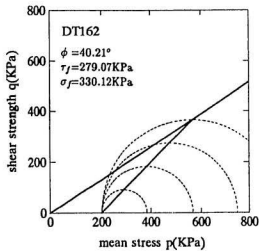
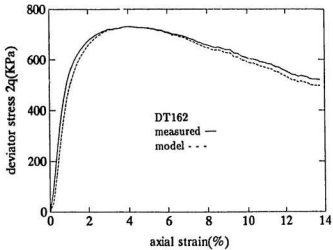


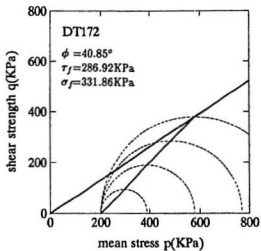
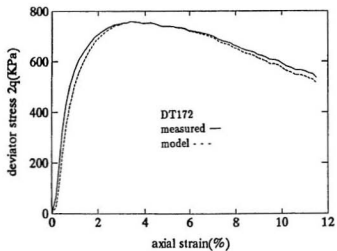


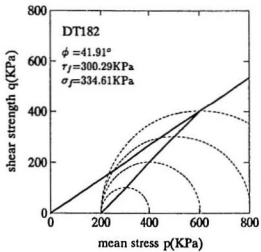
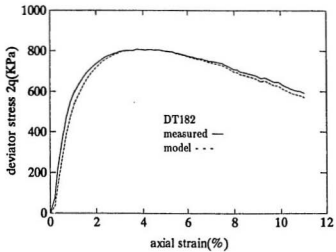


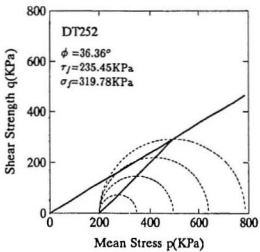
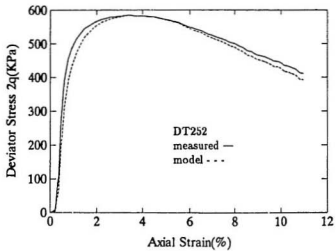


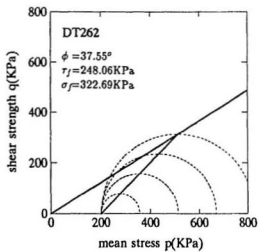
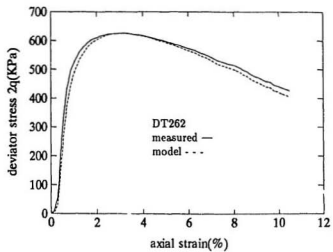


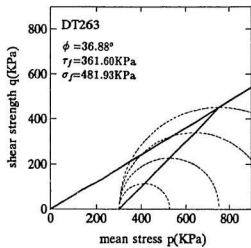
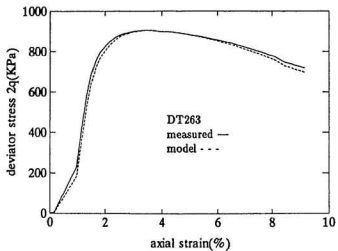


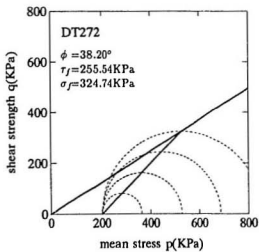
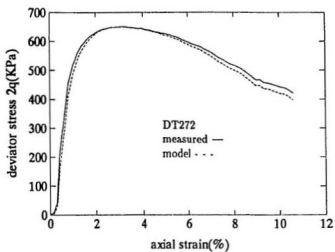


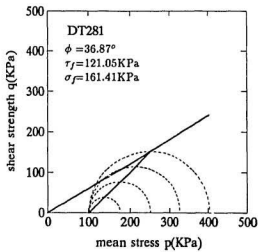
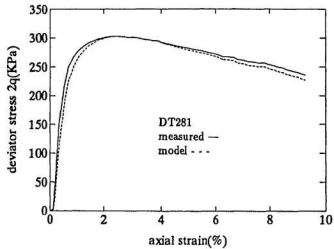


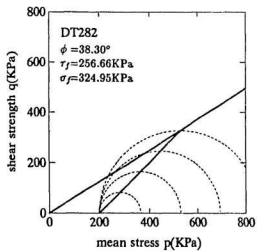
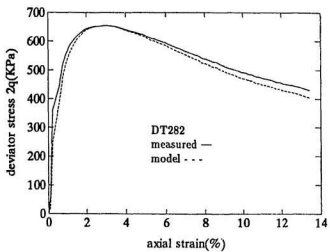


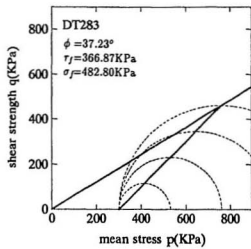
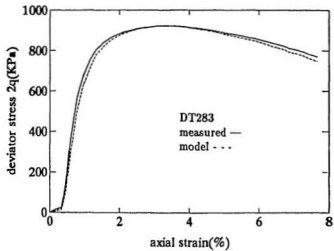


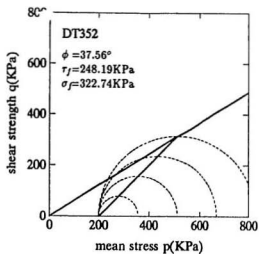
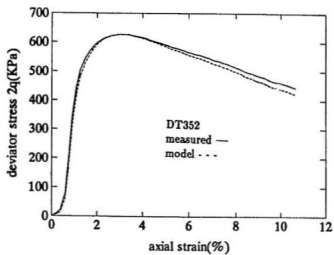


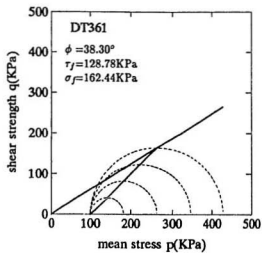
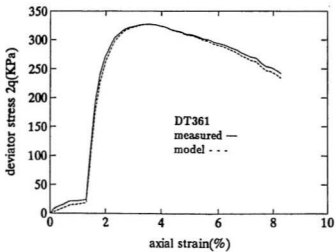


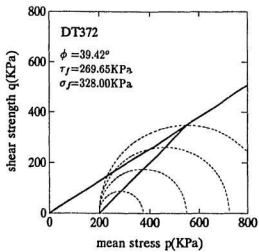
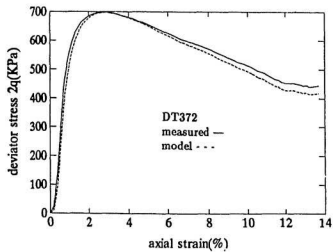










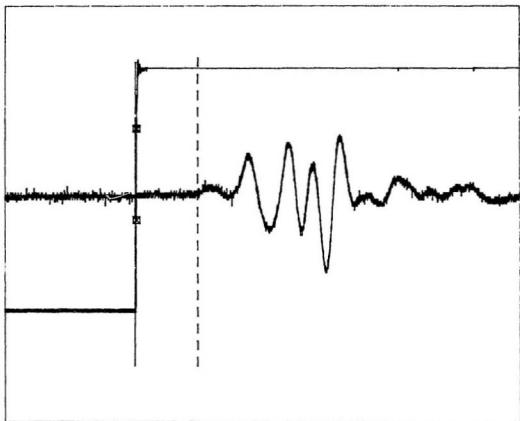


## B.2 Acoustic Data Samples

## B.2.1 measurements by oscilloscope

Test DT352

$\Delta T$  0.2520ms Trig 5.5V CH1



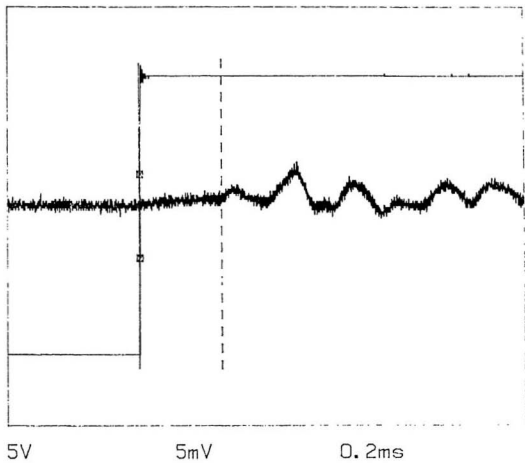
5V

5mV

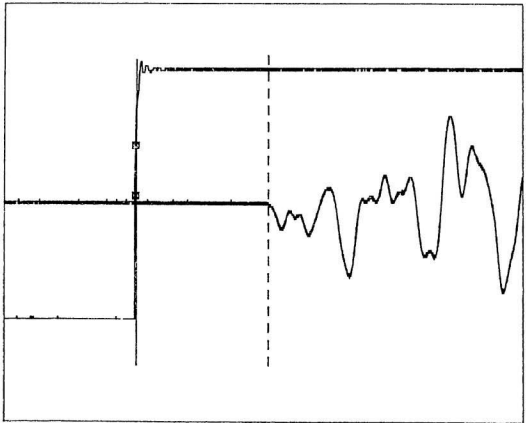
0.2ms

Test DT552

$\Delta T$  0.3220ms Trig 6.5V CH1



$\Delta T$  127.12us Trig 4.0V CH1



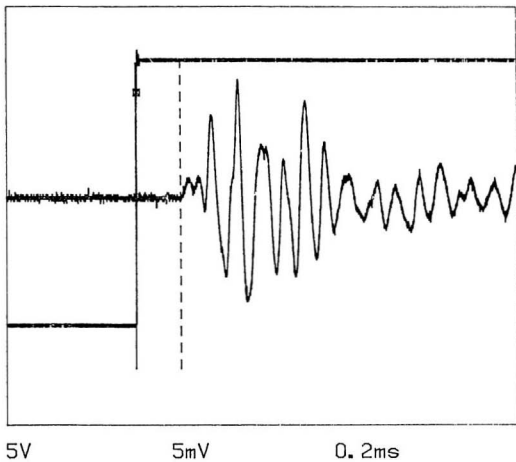
5V

10mV↓

50us

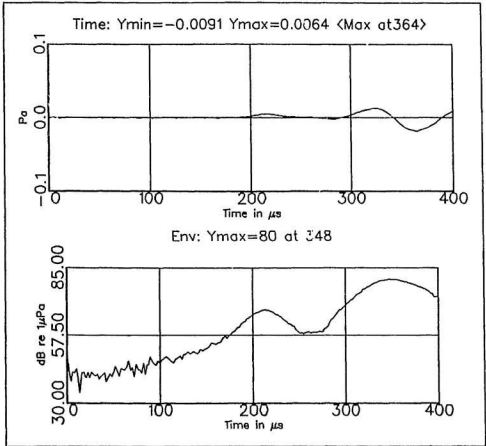
Test DT253

$\Delta T$  0.1740ms Trig 9.5V CH1

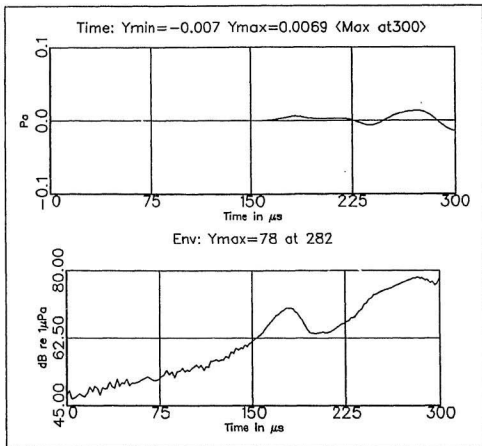


## B.2.2 measurements by Hilbert transform

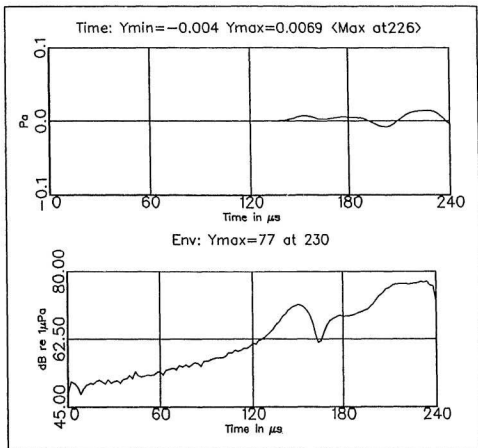
Test DT26



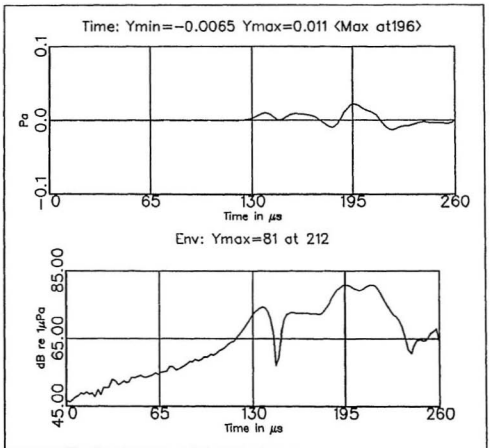
Test DT261



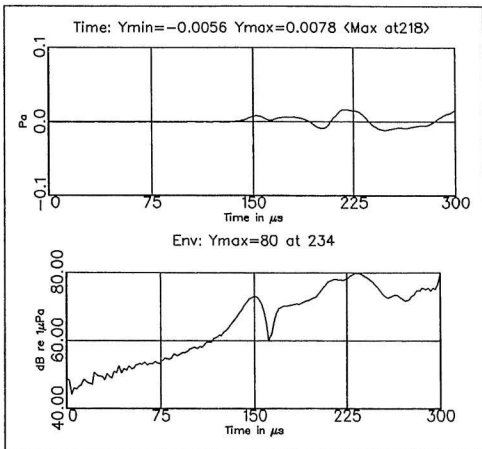
Test DT262



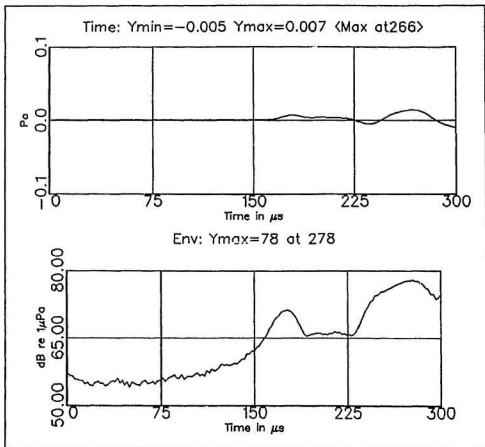
Test DT363



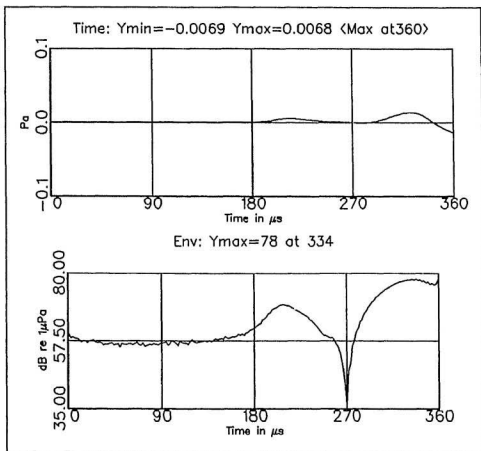
Test DT362

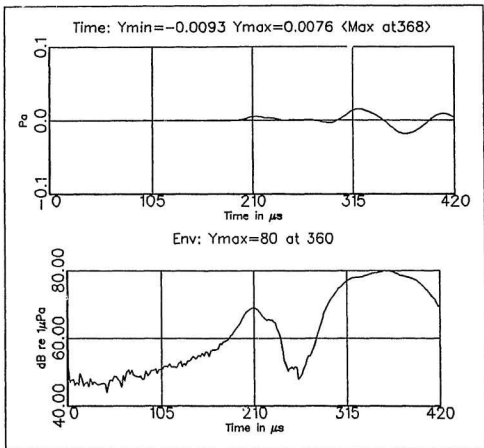


Test DT361

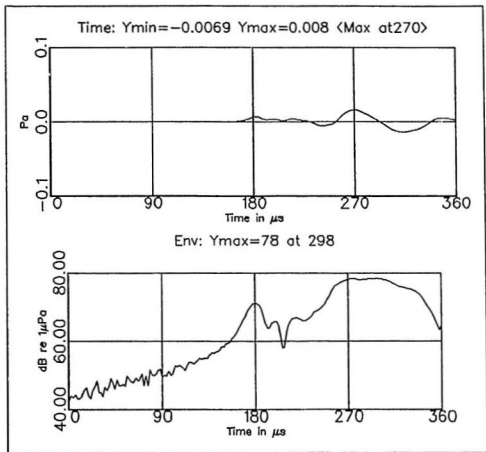


Test DT36

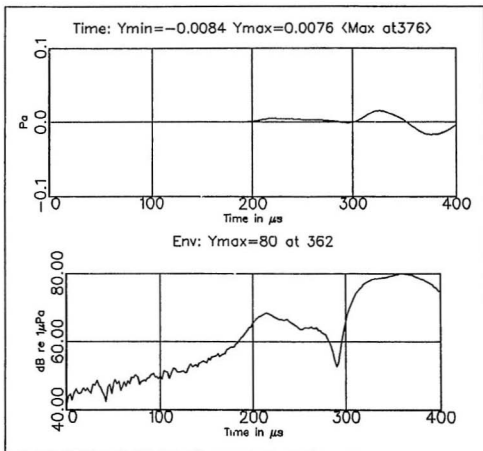




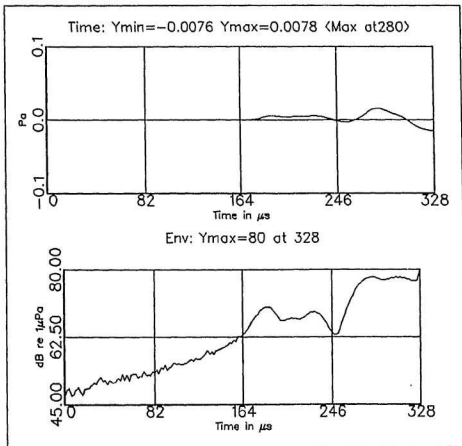
Test DT561



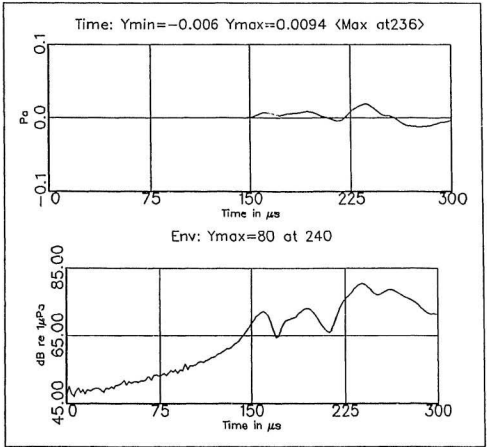
Test DT46

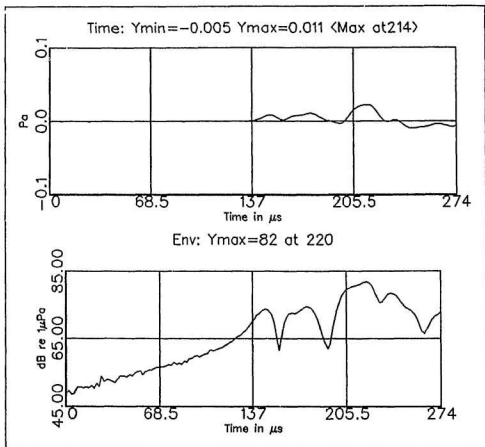


Test DT461



Test DT462





### **B.3 Stress-strain-shear wave velocity Data**

